JOC The Journal of Organic Chemistry

Article

pubs.acs.org/joc

Mechanistic and Computational Studies of Exocyclic Stereocontrol in the Synthesis of Bryostatin-like *Cis*-2,6-Disubstituted 4-Alkylidenetetrahydropyrans by Prins Cyclization

Yasuyuki Ogawa,[‡] Phillip P. Painter,[†] Dean J. Tantillo,*[,†] and Paul A. Wender*[,‡]

[†]Department of Chemistry, University of California, Davis, California 95616, United States

[‡]Departments of Chemistry and Chemical and Systems Biology, Stanford University, Stanford, California 94305-5080, United States

Supporting Information

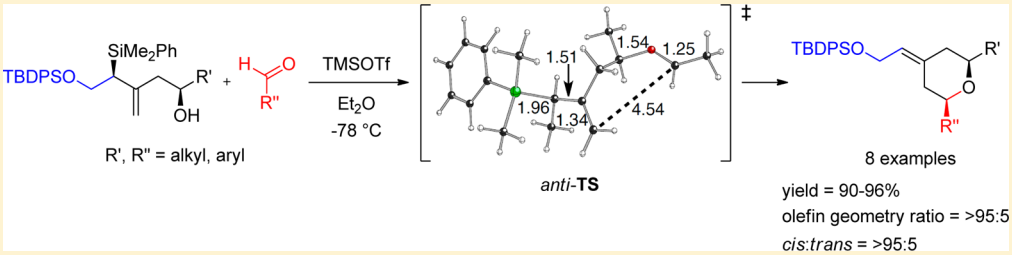

ABSTRACT: The Prins cyclization of *syn*-β-hydroxy allylsilanes and aldehydes gives *cis*-2,6-disubstituted 4-alkylidenetetrahydropyrans as sole products in excellent yields regardless of the aldehyde (R″) or *syn*-β-hydroxy allylsilane substituent (R′) used. By reversing the R″ and R′ groups, complementary exocyclic stereocontrol can be achieved. When the *anti*-β-hydroxy allylsilanes are used, the Prins cyclization gives predominantly *cis*-2,6-disubstituted 4-alkylidenetetrahydropyrans, now with the opposite olefin geometry in excellent yield. The proposed reaction mechanism and the observed stereoselectivity for these processes are supported by DFT calculations.

INTRODUCTION

Bryostatin 1 is a marine-derived macrolactone that has justifiably attracted considerable interest because of its novel structure and its initially observed antitumor activity.[1,2] It has since been found to exhibit activity in animal models of cognitive dysfunction pertinent to treatments for Alzheimer's disease[3] and in first-in-class strategies aimed at the eradication of HIV/AIDS.[4] Over 25 years ago, we initiated the first studies aimed at identifying the structural features of the bryostatin family of natural products (Figure 1) that contribute to their novel biological activities.[5] Anticipating then the challenges that would attend a practical synthesis of the natural product as well as the potential need for better leads, the purpose of our program was to use structure-based pharmacophoric hypotheses to design simpler but potentially superior functional analogues that could be synthetically accessed in a step-economical fashion.[6] In 1998, we reported the first of these designed molecules which proved to be comparable to bryostatin 1 in binding affinity to protein kinase C (PKC), a putative target mediating its activity.[7] Subsequently, second-generation analogues were prepared that were more potent than bryostatin 1 itself in binding to PKC.[8] The syntheses of these analogues were approximately 40−50 steps shorter than the reported syntheses of the natural bryostatins at the time,[9] illustrating an advantage of this function-oriented synthesis strategy.[10] Subsequently, over 100 designed analogues have been prepared in our studies with 35 exhibiting PKC affinities in the low nanomolar to picomolar range, i.e., comparable to or better than bryostatin 1.[2b] Our lead, designed analogues exhibit potent functional activity in cellular studies related to Alzheimer's disease,[3c] HIV/AIDS eradication,[11] and cancer cell apoptosis[12] and in animal models of cancer involving suppression of MYC-oncogene induced lymphoma.[13] Further underscoring the potential value of these designed agents, patient accrual in a recent bryostatin lymphoma clinical trial was terminated early "given the more potent bryostatin analogs in development"[14] in our laboratory.

One of our earlier bryostatin pharmacophore hypotheses was that the lactone carbonyl, C19 hydroxyl, and C26 hydroxyl groups contact the protein target (PKC) and thus influence binding affinity and that the A- and B-rings serve to control the correct spatial array of these pharmacophoric contacts.[5] This analysis suggests that simplifications could be made in the A- and B-rings of bryostatin without significantly changing affinity and it thus opens this approach up to synthesis-informed design of A- and B-ring simplified systems. Toward this end, in the design of our first-generation analogues, we took the liberty of removing all unnecessary A- and B-ring appendages and replaced the C14 carbon of the B-ring pyran with an oxygen atom to allow for macrocycle formation through a then-

Special Issue: Robert Ireland Memorial Issue

Received: September 14, 2012
Published: November 2, 2012

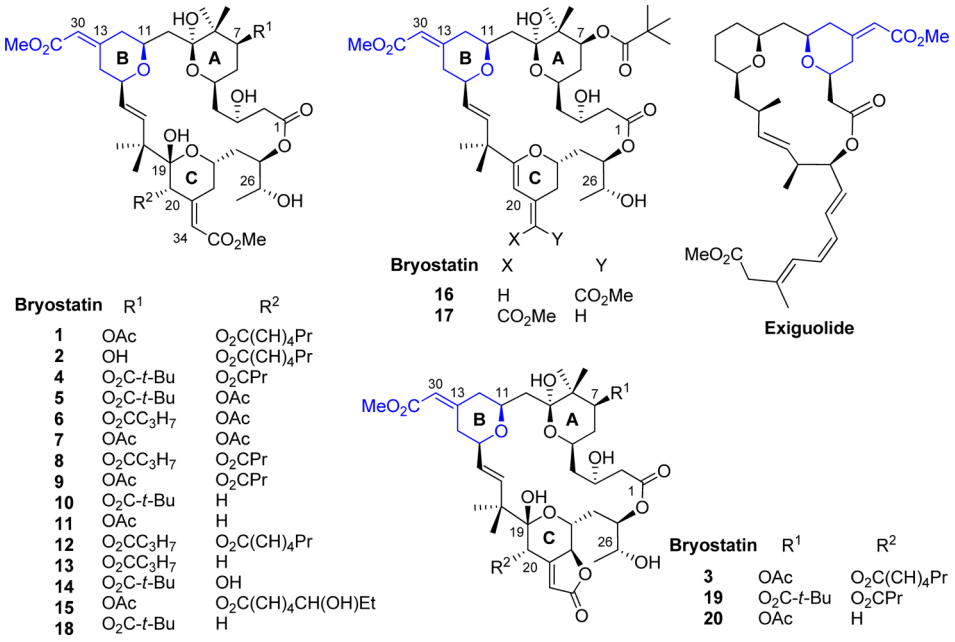

Figure 1. Bryostatins and exiguolide, examples of (*E*)- and (*Z*)-alkylidene-*cis*-2,6-disubstituted pyrans.

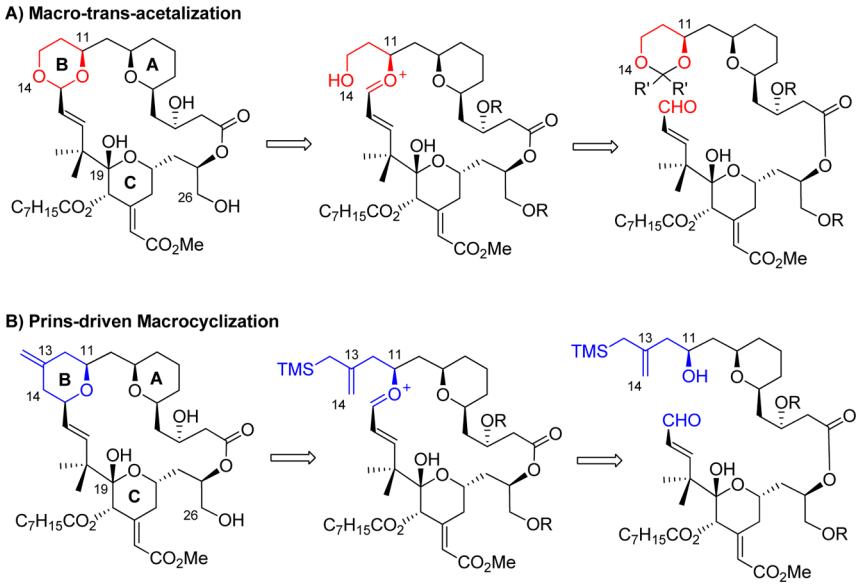

Figure 2. Ring-forming macrocyclizations.

unexplored macrotransacetalization in which an oxo-carbenium ion intermediate is trapped by a nucleophilic C14 hydroxyl group to form a B-ring dioxane (Figure 2). This strategy allowed step-economical access to analogues with bryostatin-like potency.[7,8,15] Recognizing that the nucleophilic oxygen in this strategy could be replaced by a nucleophilic C14 carbon of a C13−C14 alkene, we next explored whether a Prins-driven macrocyclization could be used in place of our macrotransacetalization to access macrocycles now with a pyranyl B-ring.[16] The Marko group reported impressive early examples of an *intermolecular* allyl silane driven Prins reaction (a.k.a. silyl-modified Sakurai reaction) for pyran synthesis,[17] and this *intermolecular* process was later used effectively in the Keck group approach to bryostatin analogues.[18] This intermolecular process has also been creatively deployed in syntheses of other natural systems.[9e,g,19] Our own work provided the first investigation of whether this process could be used *intramolecularly* to form macrocycles incorporating pyran rings. This novel Prins-driven macrocyclization strategy proved highly effective and was used in the preparation of bryostatin analogues (bryologs)[11,20] and bryostatin 9.[9f] Concurrent studies from several laboratories provided additional and impressive examples of the utility of this Prins-driven macrocyclization in accessing a wide range of natural products with pyranyl subunits.[21]

In the course of the above studies, it became apparent that while much impressive effort has gone into studies on various aspects of the Prins reaction,[22] little is known about its use in controlling exocyclic alkylidene stereochemistry. This synthetic problem is encountered in exocyclic unsaturated esters associated with the B- and C-rings of natural bryostatins, some bryostatin analogues, and other natural products such as

dx.doi.org/10.1021/jo301953h | J. Org. Chem. 2013, 78, 104−115

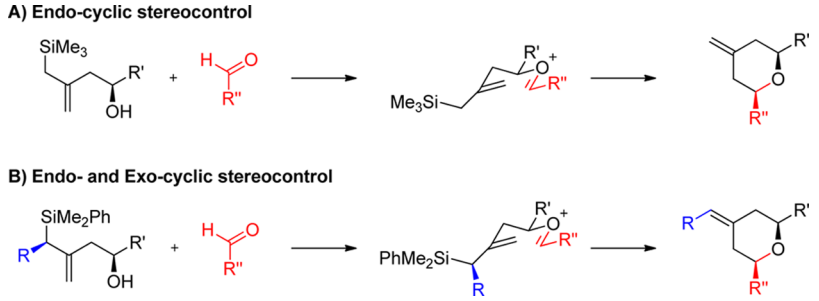

Figure 3. Silyl-terminated Prins cyclizations for endocyclic and endo- and exocyclic stereocontrol.

Scheme 1. Synthetic Route to β-Hydroxy Allylsilanes 9−12

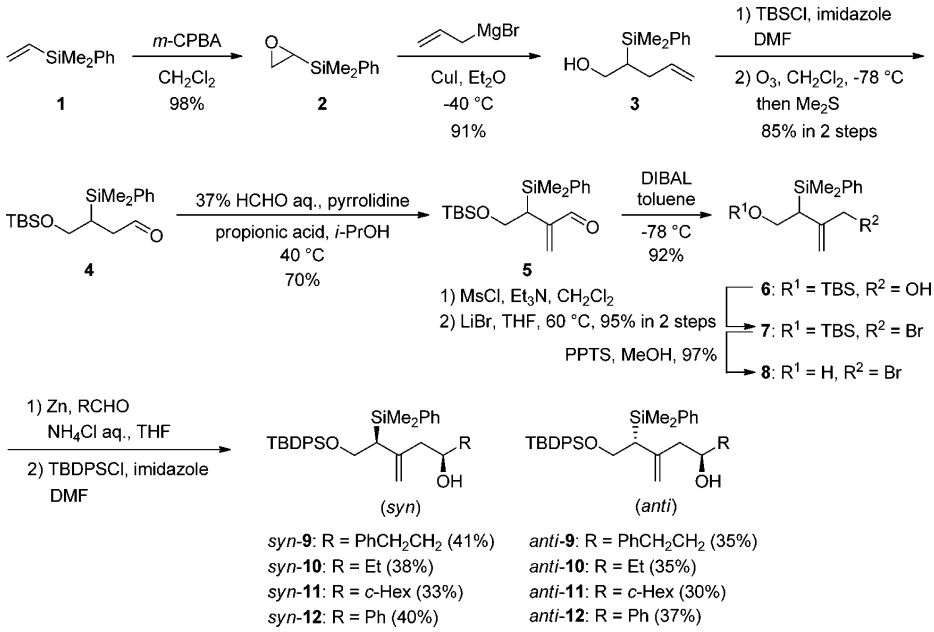

exiguolide (Figure 1). The bryostatin B-ring problem is especially challenging as the atoms flanking the C13 exocyclic alkene are virtually identical, thus providing no steric or electronic bias to control alkene geometry. Indeed direct olefination of a C13 carbonyl of a pyranone proceeds with no selectivity.[20] Current approaches to this problem preset the alkene geometry before formation of the pyran ring[23] or use reagent-controlled strategies to set the geometry after pyran formation.[24] A third general approach to this problem is to set alkene geometry during the course of pyran formation,[25] a result that could be realized, for example, if the stereogenic center of an allylic silane[26] were to control alkene geometry during a silyl-terminated Prins cyclization (Figure 3). More specifically, if the silyl-terminated Prins cyclization were to proceed by capture of a *trans*-oxocarbenium ion exclusively through either an *anti*-S_E' or *syn*-S_E' process,[27] then control of the exocyclic double bond would be achieved. If these pathways compete or if both *cis*- and *trans*-oxocarbenium ions participate, mixtures of *E*- and *Z*-alkenes would be obtained. We report herein synthetic, mechanistic and computational studies on this unexplored strategy.

RESULTS AND DISCUSSION

To evaluate this concept, we prepared the *syn*- and *anti*-β-hydroxy allylsilanes **9**−**12** through a conventional but scalable route as given in Scheme 1. Epoxidation of **1** with *m*-CPBA[28] followed by treatment with allyl cuprate gave racemic hydroxyl silane **3**.[29] Alcohol **3** was protected with TBSCl and then treated with O_3 followed by Me_2S to give aldehyde **4** in 85% yield in two steps. Introduction of an α-methylene group with formaldehyde[30] followed by reduction gave alcohol **6**, which was converted to the allylic bromide **8** by mesylation, bromide displacement, and deprotection. Allylic zinc bromide was generated in situ from allylic bromide **8** and zinc powder and then reacted individually with four different aldehydes to provide after protection *syn*- and *anti*-diastereomers **9**−**12**. These allylations proceeded with little stereoselectivity as desired because both diastereomers were required in this study. The aldehydes were selected on the basis of anticipated synthetic situations involving this process and include conjugated and nonconjugated aldehydes as well as straight chain and branched chain aldehydes. The diastereomers **9**−**12** were separated using silica gel chromatography. The stereochemistry of *syn*- and *anti*-**12** was determined by ^{1}H NMR and by transformation to the cyclic derivatives as shown in Scheme 2. For the determination of the stereochemistry of **12**, the mixture of diastereomers of 1,5-diol **13** was separated using silica gel chromatography to give **13a** and **13b**. Individual tosylation of **13a** and **13b** proceeded with a 1,2-silicon shift to give tetrahydrofurans **14a** and **14b**, respectively. The stereochemistry of each compound was confirmed by NOE experiments, indicating that **14a** has a *cis* configuration and

dx.doi.org/10.1021/jo301953h | J. Org. Chem. 2013, 78, 104−115

Scheme 2. Assignment of Relative Stereochemistry of *β*-Hydroxy Allylsilane 12

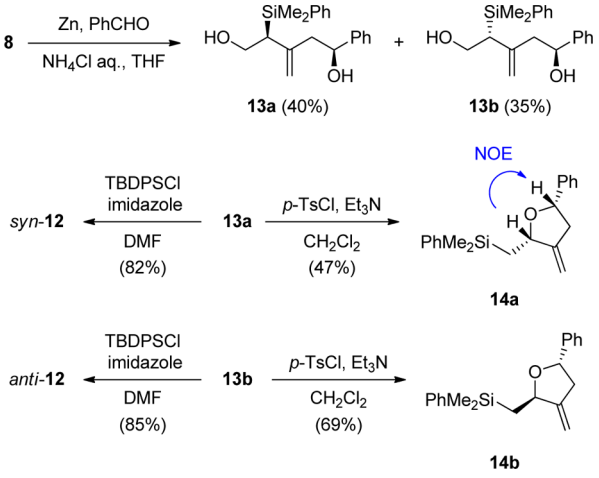

14b has a *trans* configuration. This indicates that **13a** has the *syn*-configuration and **13b** has the *anti*-configuration. Finally, to confirm the stereochemistry of **12**, **13a** and **13b** were converted to *syn*-**12** and *anti*-**12**, respectively. The relative stereochemistry of the other *β*-hydroxy allylsilanes **9**−**11** was determined by comparison of their ^{1}H NMR spectra with that of **12**.

Our initial studies focused on the Prins cyclization of the *syn*-*β*-hydroxy allylsilanes. Prins cyclization reaction using *syn*-**9** and propionaldehyde proceeded smoothly with TMSOTf in Et_2O at −78 °C to give within 1 h **15a** as the sole product in excellent yield (Table 1, entry 1). No other diastereomers were detected.

Table 1. Prins Cyclization of *syn*-*β*-Hydroxy Allylsilane 9 with Representative Aldehydes

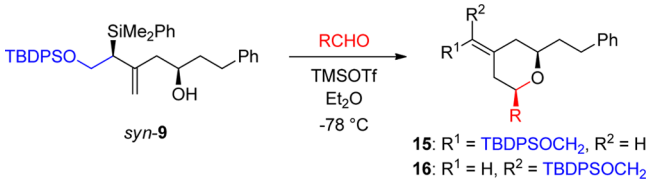

entry	R	time (h)	product	yield (%)	**15**:**16**[a]
1	Et	1	**15a**	96	>95:5
2	*c*-Hex	1	**15b**	93	>95:5
3	*t*-Bu	4	**15c**	90	>95:5
4	Ph	1	**15d**	92	>95:5
5	(*E*)-PhCH=CH	1	**15e**	95	>95:5

[a]Product ratios were determined by ^{1}H NMR.

The *cis*-disposition of the C2 and C6 substituents and the *E* geometry of the exocyclic alkene in **15a** were established by NOE experiments (Figure 4). The results for several additional examples are provided in Table 1. Branched (entries 2 and 3), sterically encumbered (entry 3), aryl-conjugated (entry 4), and styryl-conjugated (entry 5) aldehydes behaved similarly upon reaction with *syn*-**9**, providing exclusively *cis*-pyranyl products **15b**−**e** with a single exocyclic geometry in high yields and with high selectivities. Even pivalaldehyde reacted smoothly albeit somewhat less rapidly to give the cyclized product (entry 3).

We next examined the effect of variations in the substituents of the *syn*-*β*-hydroxy allylsilanes with a fixed aldehyde, 3-phenylpropionaldehyde (Table 2). Normal alkyl (*syn*-**10**), branched (*syn*-**11**), and aryl (*syn*-**12**) substituted systems each

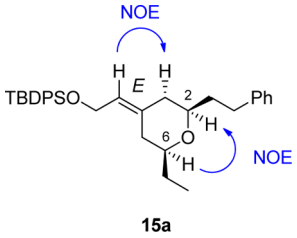

Figure 4. Relative stereochemistry of **15a**.

Table 2. Substituents Effects in the Prins Cyclization of *syn*-*β*-Hydroxy Allylsilanes 10−12 with 3-Phenylpropionaldehyde

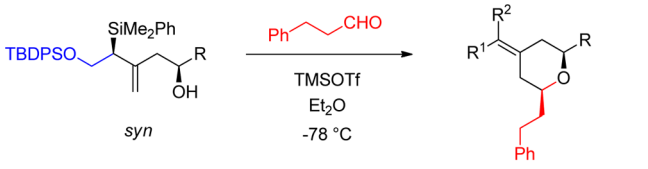

entry	allylsilane	R	time (h)	product	yield (%)	**16**:**15**[a]
1	*syn*-**10**	Et	1	**16a**	96	>95:5
2	*syn*-**11**	c-Hex	1	**16b**	95	>95:5
3	*syn*-**12**	Ph	1	**16d**	93	>95:5

[a]Product ratios were determined by ^{1}H NMR.

reacted to give the cyclized products in high yields and with high selectivities. The comparative results of Tables 1 and 2 show that one can form either **15a**,**b**,**d** or **16a**,**b**,**d** in a highly selective fashion. This strategy thus allows for the highly selective synthesis of *cis*-2,6-disubstituted pyrans with either an *E*- or *Z*-exocyclic alkene by the judicious selection of starting materials.

Our focus turned next to the Prins cyclization using *anti*-*β*-hydroxy allylsilanes. As before, the Prins cyclization reaction using *anti*-**9** and propionaldehyde with TMSOTf at −78 °C was examined first (Table 3, entry 1). The reaction proceeded smoothly and in high yield but now gave two diastereomers in a 16:84 ratio favoring **16a** over **15a**. The lower diastereoselectivity obtained with the *anti* substrate relative to the *syn* substrate in this process could arise from epimerization of the product under the reaction conditions. However, the possibility

Table 3. Prins Cyclization Using *anti*-*β*-Hydroxy Allylsilane 9 with Representative Aldehydes

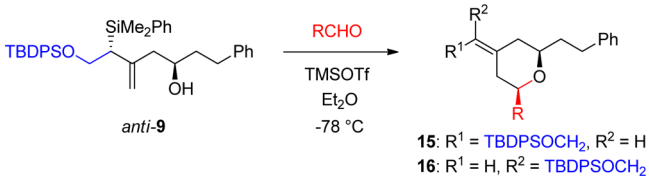

entry	R	time (h)	product	yield (%)[a]	**15**:**16**[b]
1	Et	1	**15a**, **16a**	95	16:84
2	*c*-Hex	1.5	**15b**, **16b**	95	16:84
3	*t*-Bu	8	**15c**, **16c**	80	8:92
4	Ph	1	**16d**	89	5:>95
5	(*E*)-PhCH=CH	1	**15e**, **16e**	94	6:94

[a]Combined isolated yield. [b]Product ratios were determined by ^{1}H NMR.

dx.doi.org/10.1021/jo301953h | *J. Org. Chem.* 2013, 78, 104−115

of epimerization was discounted by two experiments. When product **16a** was treated with TMSOTf, no isomerization was observed. Moreover, when the reaction was monitored by ^{1}H NMR at 10, 30, and 60 min, the product ratio remained constant. The results obtained with other aldehydes are provided in Table 3. In general, the reactions proceeded in very good to high yields for all aldehydes. The reactions were somewhat slower for *anti*-**9** and branched aldehydes (entries 2 and 3) than for *syn*-**9** with the same aldehydes. All reactions provided **16** as main product with **15** as minor product, i.e., the stereochemical complement of the selectivity observed when *syn*-**9** was used (Table 1). When pivalaldehyde was used, the selectivity of olefin geometry was increased (entry 3). Higher selectivity was also observed when aromatic aldehyde and conjugated aldehyde were used (entries 4 and 5). When benzaldehyde was used, only one diastereomer (**16d**) was obtained.

We next examined the effect of variations in the substituents of the *anti*-β-hydroxy allylsilanes with a common aldehyde (Table 4). The ethyl- and cyclohexyl-substituted β-hydroxy

Table 4. Substituents Effects in the Prins Cyclization of *anti*-β-Hydroxy Allylsilanes 10−12 with 3-Phenylpropionaldehyde

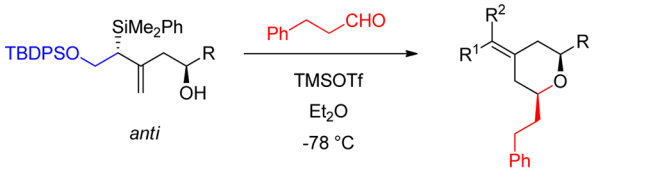

16: R^1 = $TBDPSOCH_2$, R^2 = H
15: R^1 = H, R^2 = $TBDPSOCH_2$

entry	allylsilane	R	time (h)	product	yield (%)	**16:15**[a]
1	*anti*-**10**	Et	1	**15a**, **16a**	94	18:82
2	*anti*-**11**	c-Hex	3	**15b**, **16b**	95	21:79
3	*anti*-**12**	Ph	8	**15d**, **16d**	79	8:92

[a]Combined isolated yield. [b]Product ratios were determined by ^{1}H NMR.

allylsilanes reacted in good yields but with moderate selectivities (Table 4, entries 1 and 2) while the phenyl substituted system gave better selectivity but a lower yield (entry 3). In all cases, only the *cis*-2,6-disubstituted products are obtained. However, in contrast to the reactions using *syn*-β-hydroxy allylsilanes, the yields and selectivities for the reaction of *anti*-β-hydroxy allylsilanes are more sensitive to coreactant aldehydes and substituents.

To probe the mechanism of this reaction and the origin of observed stereoselectivity, density functional theory (DFT) calculations were carried out for model *syn*-β-hydroxy allylsilane **I** (Figure 5) and its *anti*-β-hydroxy allylsilane analogue (Figure 6b, R = R′ = Me). It was found that cyclization and loss of the silyl group occur in separate steps, although the barriers for these steps are predicted to be small. In the first step, there are two possible cyclization modes (*anti* and *syn*; *syn* is defined here as the silicon group being oriented toward the forming C−C bond in the transition state structure) that take advantage of hyperconjugation between the C−Si σ-bond and the C═C π-bond. The transition-state structures for cyclization, *anti*-**TS1**, and *syn*-**TS1** are quite early (not surprising, given the exothermicity/exergonicity of the cyclizations), with the motion associated with their imaginary frequencies corresponding primarily to rotation around the internal O−C σ-bond. This rotation brings the C═C and C═O π-bonds into proximity, and their coupling occurs without an additional barrier (note that chairlike structures are encountered along these reaction coordinates once the initial conformational change is complete).[31] Interconversion of **III** and **IV** is associated with a comparatively large barrier (through a transition state structure for which β-silyl stabilization is lost), suggesting that stereochemical scrambling at this stage is unlikely. The loss of the silyl group in the second step, modeled here using an attacking solvent molecule (dimethyl ether for simplicity) is also predicted to be facile, but the inherent preference for an *anti* silyl group is maintained in the corresponding transition state structures (*anti*- and *syn*-**TS2**) and the minima preceding them (Figure 5, bottom).

Given these results, it appears that the stereoselectivity of the Prins cyclization is determined by the energy difference between the transition-state structures for cyclization (*anti*-**TS1** and *syn*-**TS1**), although the preference for an *anti* silyl group is maintained throughout the reaction. For the *syn*-β-hydroxy allylsilane model **I**, the predicted difference in energy between *anti*-**TS1** and *syn*-**TS1** is 1.6 kcal mol^{-1}, favoring the transition-state structure leading to the experimentally observed product. When the analogous *anti*-β-hydroxy allylsilane model with MeCHO (Figure 6b, R = R′ = R″ = Me) is used, the predicted energy difference between the *anti* and *syn* transition state structures for cyclization is only 0.5 kcal mol^{-1}, which is consistent with the observation of decreased selectivity for *anti*-β-hydroxy allylsilane reactants.

The selectivity for these Prins cyclizations can be rationalized through a combination of simple steric and electronic effects. For *syn*-β-hydroxy allylsilanes (Figure 6a), cyclization occurs through chairlike structures in which the alkyl substituent occupies an equatorial position. Second, the SiR_3 group aligns itself perpendicular to the C═C π-bond to maximize the incipient β-silyl stabilization. The *anti* arrangement is preferred, which places the alkyl group α to the silyl on the side of the molecule where the new σ-bond forms. The situation is the same for *anti*-β-hydroxy allylsilanes (Figure 6b), except that the α-alkyl group now resides on the side of the molecule away from the forming bond. This environment is more sterically crowded, resulting in a diminution of the preferences for an *anti* silyl group: with $C_\alpha H_2$ rather than $C_\alpha H(CH_3)$ the preference for *anti* is predicted to be 2.5 kcal mol^{-1} which is reduced upon replacing one or the other hydrogen with a methyl group. Truncation of the *anti* and *syn* cyclization transition state structures for the system with $C_\alpha H_2$ to $Ph(CH_3)_2SiCH_2$vinyl groups and recalculation of their energies (without optimization of their geometries) indicated that the preference for the *anti* arrangement is almost entirely localized to this structural unit (i.e., the *anti* preference for the truncated system ≈ the *anti* preference for the full system). It appears that in order to reduce steric clashes in the *syn* transition state structure, the Si−C_α−C_β═C dihedral angle deviates from 90° (this dihedral angle is predicted to be 91° in the *anti* transition state structure, but −67° in the *syn* transition state structure), leading to a reduction in hyperconjugation between the C−Si σ-bond and the C═C π-bond. This diminished interaction is manifested in a slight reduction of the Si−C_α bond length (by 0.1 Å), a slight elongation of the C_α−C_β bond length (by 0.05 Å) and an opening of the Si−C_α−C_β angle (by 3°).[32]

dx.doi.org/10.1021/jo301953h | J. Org. Chem. 2013, 78, 104−115

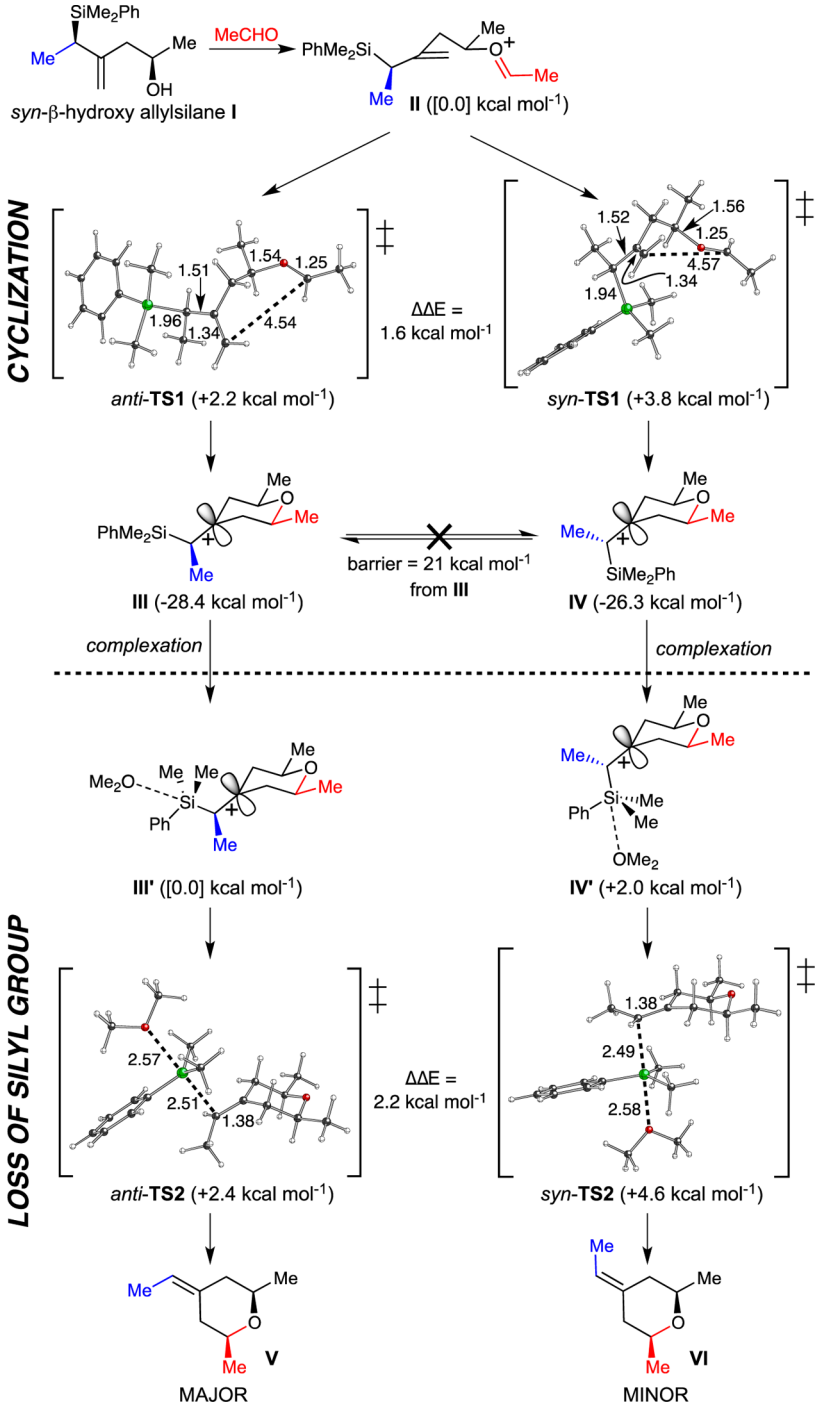

Figure 5. Mechanism for the Prins cyclization with *syn*-*β*-hydroxy allylsilane proposed on the basis of computational results. Relative energies shown were computed with B3LYP/6-31+G(d,p)//B3LYP/6-31G(d).

CONCLUSION

In conclusion, we have shown that the silyl-terminated Prins cyclization can be used to control both endocyclic and exocyclic stereochemistry, thus providing selective access to *cis*-2,6-disubstituted tetrahydropyrans with either a (*Z*)- or (*E*)-4-alkylidene group. The influence of the relative stereochemistry of silicon and oxygen-bearing chiral centers of the *β*-hydroxy allylsilanes on the product geometry in Prins cyclization has been established experimentally and supported computationally. When the *syn*-*β*-hydroxy allylsilanes were used, the Prins cyclization gave *cis*-2,6-disubstituted 4-alkylidenetetrahydropyrans as the sole products in excellent yields. The olefin geometry is set with high selectivity regardless of the aldehydes and the substituents of the *syn*-*β*-hydroxy allylsilanes used. When the *anti*-*β*-hydroxy allylsilanes were used, the Prins cyclization gave predominantly *cis*-2,6-disubstituted 4-alkylidenetetrahydropyrans, now with the opposite olefin geometry in excellent yield. The proposed reaction mechanism and the observed stereoselectivity for this reaction are consistent with results from the DFT calculations. This strategy can provide stereoselectively both (*E*)- and (*Z*)-*cis*-2,6-disubstituted 4-alkylidenetetrahydropyrans as required to access natural bryostatins and their

dx.doi.org/10.1021/jo301953h | J. Org. Chem. 2013, 78, 104−115

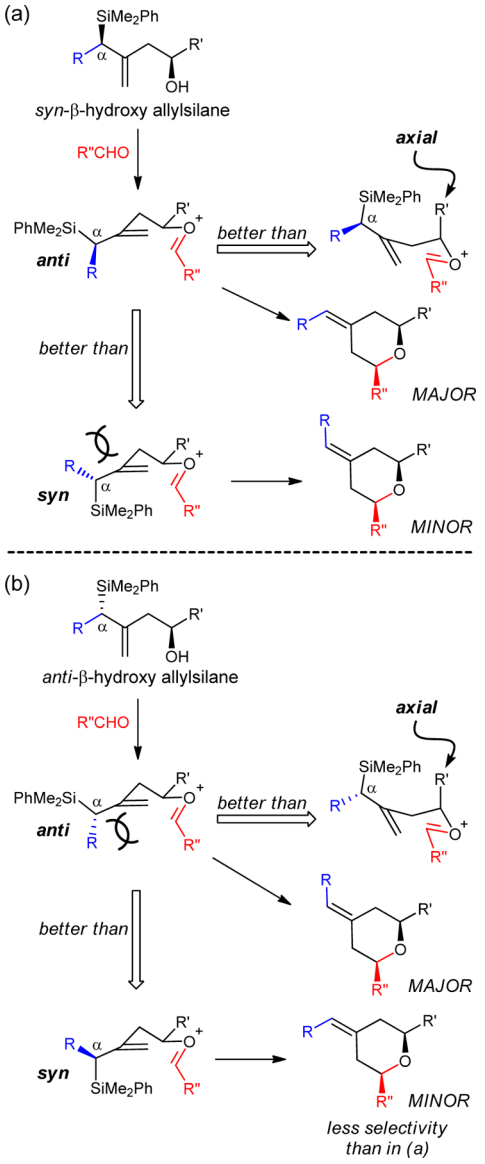

Figure 6. Model for rationalizing observed selectivity.

structural and functional analogues as well as other pyranyl targets.

EXPERIMENTAL SECTION

General Procedures. All reactions were run under a N_2 atmosphere in flame- or oven-dried glassware. Reactions were stirred using Teflon-coated magnetic stirrer bars. Reactions were monitored using thin-layer silica gel chromatography (TLC) using 0.25 mm silica gel 60F plates with fluorescent indicator. Plates were visualized by treatment with UV, acidic *p*-anisaldehyde stain, $KMnO_4$ stain with gentle heating. Products were purified by silica gel (230−400 mesh) column chromatography using the solvent systems indicated. When necessary, solvents and reagents were purified before use. THF was distilled from sodium benzophenone ketyl under N_2. CH_2Cl_2, Et_2O, and toluene were passed through an alumina drying column using N_2 pressure. Et_3N was distilled from CaH_2 under N_2. All other reagents were purchased from commercial supplies and were used as received without additional purification. NMR spectra were measured on magnetic resonance spectrometers (^{1}H at 500, 400 MHz, ^{13}C at 125, 100 MHz), as noted. ^{1}H chemical shifts are reported relative to the residual solvent peak (chloroform = 7.26 ppm; benzene = 7.15 ppm) as follows: chemical shift (δ), (multiplicity (s = singlet, d = doublet, t = triplet, br = broad), coupling constant(s) in Hz, integration). ^{13}C chemical shifts are reported relative to the residual deuterated solvent ^{13}C signals ($CDCl_3$ = 77.1, C_6D_6 = 128.0 ppm). Infrared spectra were recorded on a Fourier transform spectrometer (FTIR) and are reported in wavenumbers (cm^{-1}). High-resolution mass spectra were recorded on a hybrid quadrupole time-of-flight (Q-Tof) LC/MS instrument.

2.[28] ^{1}H NMR (400 MHz, $CDCl_3$): δ = 7.59−7.53 (m, 2H), 7.41−7.33 (m, 3H), 2.93 (t, J = 5.6 Hz, 1H), 2.56 (dd, J = 5.6, 4.0 Hz, 1H), 2.39 (dd, J = 5.2, 4.0 Hz, 1H), 0.36 (s, 3H), 0.31 (s, 3H). ^{13}C NMR (100 MHz, $CDCl_3$): δ = 136.0, 134.0, 129.6, 128.0, 44.7, 43.6, −5.2, −5.5. IR (thin film): 3047, 2959, 1428, 1315, 1250, 1232, 1117 cm^{-1}.

3.[29] ^{1}H NMR (400 MHz, $CDCl_3$): δ = 7.56−7.50 (m, 2H), 7.39−7.34 (m, 3H), 5.90−5.78 (m, 1H), 5.08−5.02 (m, 1H), 5.01−4.95 (m, 1H), 3.79 (ddd, J = 10.8, 6.0, 4.4 Hz, 1H), 3.69 (ddd, J = 10.8, 7.2, 5.2 Hz, 1H), 2.36−2.27 (m, 1H), 2.22−2.10 (m, 1H), 1.42 (dd, J = 6.0, 5.2 Hz, 1H), 1.29−1.21 (m, 1H), 0.35 (s, 6H). ^{13}C NMR (100 MHz, $CDCl_3$): δ = 139.5, 138.0, 133.9, 129.2, 127.9, 115.5, 63.8, 32.3, 30.2, −3.6, −3.8. IR (thin film): 3369, 3070, 2956, 2903, 1638, 1427, 1250, 1156, 1111 cm^{-1}.

4. To a solution of **3** (4.65 g, 21.1 mmol) in DMF (50 mL) were added TBSCl (3.80 g, 25.1 mmol) and imidazole (3.44 g, 50.6 mmol). The mixture was stirred at rt for 1 h and diluted with water and Et_2O. The separated aqueous phase was extracted with Et_2O, and the combined organic solutions were washed with brine, dried with Na_2SO_4, and concentrated in vacuo to give crude TBS ether, which was used in the next step without further purification. The crude TBS ether was dissolved in CH_2Cl_2 (100 mL). The solution was cooled to −78 °C and treated with ozone until the solution turned light blue. The reaction was quenched at −78 °C with dimethyl sulfide (3.10 mL, 42.2 mmol), warmed to rt, stirred for 12 h, and concentrated in vacuo. The residual oil was purified by column chromatography (silica gel, 0%→10% EtOAc/pentane) to give **4** (6.05 g, 85% yield in two steps) as a colorless oil. R_f (pentane/EtOAc 10/1) = 0.63. ^{1}H NMR (400 MHz, $CDCl_3$): δ = 9.68 (dd, J = 3.2, 1.2 Hz, 1H), 7.53−7.46 (m, 2H), 7.40−7.32 (m, 3H), 3.76 (dd, J = 10.0, 4.0 Hz, 1H), 3.58 (dd, J = 10.0, 8.0 Hz, 1H), 2.43 (ddd, J = 16.8, 10.4, 3.2 Hz, 1H), 2.33 (ddd, J = 16.8, 4.0, 1.2 Hz, 1H), 1.82−1.74 (m, 1H), 0.86 (s, 9H), 0.34 (s, 3H), 0.33 (s, 3H), −0.01 (s, 3H), −0.01 (s, 3H). ^{13}C NMR (100 MHz, $CDCl_3$): δ = 203.5, 137.1, 133.9, 129.4, 128.0, 63.8, 42.4, 26.0, 25.4, 18.3, −3.9, −4.2, −5.50, −5.52. IR (thin film): 3070, 2955, 2857, 2712, 1725, 1471, 1428, 1253, 1094 cm^{-1}. HRMS (ESI+, m/z): calcd for $C_{18}H_{32}NaO_2Si_2$ $[(M + Na)]^+$ 359.1833, found 359.1833.

5. To a mixture of aqueous formaldehyde solution (37% formaldehyde in water, 1.45 mL, 17.9 mmol) and **4** (6.0 g, 17.9 mmol) in *i*-PrOH (4 mL) were added propionic acid (132 mg, 1.79 mmol) and pyrrolidine (127 mg, 1.79 mmol). The reaction mixture was stirred at 45 °C for 3 h. The reaction was quenched with satd $NaHCO_3$ aq and then extracted with CH_2Cl_2. The combined extracts were washed with brine, dried with Na_2SO_4, and concentrated in vacuo. The residual oil was purified by column chromatography (silica gel, 0%→5% EtOAc/pentane) to give **5** (4.40 g, 70% yield) as a colorless oil. R_f (pentane/EtOAc 10/1) = 0.68. ^{1}H NMR (400 MHz, C_6D_6): δ = 9.21 (s, 1H), 7.50−7.44 (m, 2H), 7.24−7.12 (m, 3H), 5.85 (s, 1H), 5.38 (s, 1H), 3.77 (dd, J = 10.0, 7.6 Hz, 1H), 3.72 (dd, J = 10.0, 4.8 Hz, 1H), 2.93 (dd, J = 7.2, 4.8 Hz, 1H), 0.89 (s, 9H), 0.29 (s, 3H), 0.27 (s, 3H), −0.06 (s, 3H), −0.07 (s, 3H). ^{13}C NMR (100 MHz, C_6D_6): δ = 193.6, 150.8, 137.2, 134.4, 132.1, 129.4, 128.0, 63.8, 31.0, 26.1, 18.4, −3.0, −4.1, −5.39, −5.43. IR (thin film): 3071, 2955, 2857, 1693, 1612, 1471, 1253, 1087 cm^{-1}. HRMS (ESI+, m/z): calcd for $C_{19}H_{32}NaO_2Si_2$ $[(M + Na)]^+$ 371.1833, found 371.1834.

6. Compound **5** (4.40 g, 12.6 mmol) was dissolved in toluene (100 mL). The solution was cooled to −78 °C, and DIBAL in toluene (1.0 M, 25.2 mL) was added dropwise. The mixture was stirred at −78 °C for 3 h. After the reaction was quenched with MeOH, satd Rochelle's salt solution was introduced, and the heterogeneous reaction mixture was allowed to rt for 2 h. The separated aqueous phase was extracted with EtOAc, and the combined organic solutions were washed with brine, dried with Na_2SO_4, and concentrated. The residual oil was purified by column chromatography (silica gel, 10%→20% EtOAc/

dx.doi.org/10.1021/jo301953h | J. Org. Chem. 2013, 78, 104−115

pentane) to give **6** (4.06 g, 92% yield) as a colorless oil. R_f (pentane/EtOAc 10/1) = 0.18. ^{1}H NMR (400 MHz, C_6D_6): δ = 7.49−7.43 (m, 2H), 7.21−7.15 (m, 3H), 5.10 (td, J = 2.8, 0.8 Hz, 1H), 4.81 (d, J = 0.8 Hz, 1H), 3.89−3.78 (m, 4H), 2.06 (dd, J = 8.4, 5.2 Hz, 1H), 1.81 (t, J = 6.0 Hz, 1H), 0.93 (s, 9H), 0.32 (s, 3H), 0.29 (s, 3H), 0.00 (s, 3H), −0.01 (s, 3H). ^{13}C NMR (100 MHz, C_6D_6): δ = 149.7, 138.0, 134.2, 129.4, 128.0, 109.3, 67.4, 65.3, 37.0, 26.1, 18.5, −3.4, −3.8, −5.39, −5.42. IR (thin film): 3367, 3070, 2955, 2856, 1643, 1471, 1253, 1084 cm^{-1}. HRMS (ESI+, m/z): calcd for $C_{19}H_{34}NaO_2Si_2$ [(M + Na)]$^+$ 373.1990, found 373.1992.

7. To a solution of **6** (4.06 g, 11.6 mmol) and Et_3N (3.51 g, 34.8 mmol) in CH_2Cl_2 (100 mL) was added MsCl (1.98 g, 17.4 mmol) at 0 °C. The mixture was stirred at rt for 2 h, and then water was added. The separated aqueous phase was extracted with CH_2Cl_2, and the combined organic solutions were washed with brine, dried with Na_2SO_4 ,and concentrated in vacuo to give crude mesylate, which was used in the next step without further purification. To a solution of crude mesylate in THF (100 mL) was added LiBr (3.03 g, 34.8 mmol) at rt. The mixture was stirred at 60 °C for 2 h, cooled to rt, and diluted with Et_2O and H_2O. The separated aqueous phase was extracted with Et_2O, and the combined organic solutions were washed with brine, dried with Na_2SO_4, and concentrated. The residual oil was purified by column chromatography (silica gel, 0%→5% EtOAc/pentane) to give **7** (4.55 g, 95% yield in 2 steps) as a colorless oil. R_f (pentane/EtOAc 10/1) = 0.88. ^{1}H NMR (400 MHz, C_6D_6): δ = 7.48−7.42 (m, 2H), 7.21−7.15 (m, 3H), 4.96 (d, J = 0.8 Hz, 1H), 4.85 (d, J = 0.8 Hz, 1H), 3.86 (d, J = 6.0 Hz, 2H), 3.55 (dd, J = 10.0, 0.8 Hz, 1H), 3.39 (dd, J = 10.0, 0.8 Hz, 1H), 2.23 (t, J = 6.0 Hz, 1H), 0.95 (s, 9H), 0.33 (s, 3H), 0.32 (s, 3H), 0.02 (s, 3H), 0.01 (s, 3H). ^{13}C NMR (100 MHz, C_6D_6): δ = 146.5, 138.0, 134.2, 129.4, 128.0, 114.0, 65.7, 39.9, 37.1, 26.1, 18.5, −3.3, −3.6, −5.38, −5.42. IR (thin film): 3070, 2955, 2857, 1627, 1471, 1254, 1208, 1084 cm^{-1}. HRMS (ESI+, m/z): calcd for $C_{19}H_{33}BrNaOSi_2$ [(M + Na)]$^+$ 435.1146, found 435.1146.

8. To a solution of **7** (2.20 g, 5.34 mmol) in MeOH (50 mL) was added PPTS (134 mg, 0.534 mmol) at rt. The mixture was stirred at rt for 12 h. The reaction was quenched with satd $NaHCO_3$ aq and then diluted with Et_2O and H_2O. The separated aqueous phase was extracted with Et_2O, and the combined organic solutions were washed with brine, dried with Na_2SO_4, and concentrated. The residual oil was purified by column chromatography (silica gel, 10%→15% EtOAc/pentane) to give **8** (1.54 g, 97% yield) as a colorless oil. R_f (pentane/EtOAc 10/1) = 0.19. ^{1}H NMR (400 MHz, C_6D_6): δ = 7.38−7.31 (m, 2H), 7.21−7.12 (m, 3H), 4.92 (t, J = 0.8 Hz, 1H), 4.66 (s, 1H), 3.72−3.62 (m, 2H), 3.49 (dd, J = 10.0, 0.8 Hz, 1H), 3.31 (dd, J = 10.0, 0.8 Hz, 1H), 2.18 (dd, J = 8.4, 6.0 Hz, 1H), 1.25 (brs, 1H), 0.17 (s, 3H), 0.16 (s, 3H). ^{13}C NMR (100 MHz, C_6D_6): δ = 145.3, 137.2, 134.2, 129.5, 128.1, 113.9, 63.5, 39.6, 38.1, −4.1, −4.3. IR (thin film): 3401, 3069, 2957, 2878, 1626, 1427, 1250, 1209, 1112, 1048 cm^{-1}. HRMS (ESI+, m/z): calcd for $C_{13}H_{19}BrNaOSi$ [(M + Na)]$^+$ 321.0281, found 321.0276.

General Procedure for β-Hydroxy Allylsilanes. A mixture of **8** (500 mg, 1.67 mmol), zinc powder (120 mg, 1.84 mmol), and aldehyde (1.84 mmol) in THF−satd NH_4Cl aq (9.6 mL−1.6 mL) was stirred for 2 h. After dilution with Et_2O, the separated aqueous phase was extracted with Et_2O, and the combined organic solutions were dried with Na_2SO_4 and concentrated to give crude 1,5-diol. To a solution of crude 1,5-diol in DMF (8 mL) were added TBDPSCl (477 mg, 1.67 mmol) and imidazole (227 mg, 3.34 mmol). The mixture was stirred at rt for 1 h and diluted with Et_2O and H_2O. The separated aqueous phase was extracted with Et_2O, and the combined organic solutions were washed with brine, dried with Na_2SO_4, and concentrated in vacuo. The residue was purified by chromatography with EtOAc−pentane to give *syn*- and *anti*-β-hydroxy allylsilane, respectively.

syn-**9**. Colorless oil. Yield: 405 mg, 41% (in two steps). R_f (pentane/EtOAc 10/1) = 0.56. ^{1}H NMR (500 MHz, C_6D_6): δ = 7.79−7.73 (m, 4H), 7.30−7.26 (m, 2H), 7.25−7.06 (m, 14H), 5.02 (s, 1H), 4.84 (s, 1H), 4.03 (t, J = 10.5 Hz, 1H), 4.01−3.95 (m, 1H), 3.94 (dd, J = 10.5, 4.0 Hz, 1H), 3.00−2.93 (m, 2H), 2.76 (ddd, J = 14.0, 10.0, 6.5 Hz, 1H), 2.19 (dd, J = 10.5, 4.0 Hz, 1H), 2.05 (dd, J = 13.5, 10.0 Hz, 1H), 1.98−1.87 (m, 2H), 1.73−1.64 (m, 1H), 1.17 (s, 9H), 0.12 (s, 3H), 0.09 (s, 3H). ^{13}C NMR (100 MHz, C_6D_6): δ = 146.2, 143.0, 137.1, 136.02, 135.93, 134.1, 133.63, 133.60, 130.03, 130.02, 129.4, 128.9, 128.6, 128.12, 128.09, 128.0, 125.9, 111.9, 67.3, 65.4, 48.0, 39.3, 39.2, 32.8, 27.0, 19.4, −4.2, −4.8. IR (thin film): 3474, 3071, 2931, 2858, 1632, 1427, 1250, 1112, 1070 cm^{-1}. HRMS (ESI+, m/z): calcd for $C_{38}H_{48}NaO_2Si_2$ [(M + Na)]$^+$ 615.3085, found 615.3079.

anti-**9**. Colorless oil. Yield: 346 mg, 35% (in two steps). R_f (pentane/EtOAc 10/1) = 0.51. ^{1}H NMR (400 MHz, C_6D_6): δ = 7.80−7.70 (m, 4H), 7.31−7.26 (m, 2H), 7.24−7.04 (m, 14H), 4.93 (s, 1H), 4.76 (s, 1H), 4.02−3.94 (m, 2H), 3.92−3.83 (m, 1H), 3.34 (s, 1H), 2.91 (ddd, J = 13.6, 9.6, 5.2 Hz, 1H), 2.75 (ddd, J = 13.6, 9.6, 6.8 Hz, 1H), 2.59−2.51 (m, 1H), 2.12 (dd, J = 13.2, 2.8 Hz, 1H), 1.93 (dd, J = 13.2, 9.6 Hz, 1H), 1.90−1.79 (m, 1H), 1.75−1.63 (m, 1H), 1.17 (s, 9H), 0.13 (s, 3H), 0.10 (s, 3H). ^{13}C NMR (100 MHz, C_6D_6): δ = 147.9, 142.9, 137.1, 136.03, 135.96, 134.2, 133.5, 133.4, 130.1, 130.0, 129.4, 128.9, 128.6, 128.10, 128.06, 128.0, 125.9, 110.7, 72.6, 66.1, 48.2, 41.4, 39.7, 32.4, 26.9, 19.3, −4.0, −5.0. IR (thin film): 3459, 3070, 2931, 2858, 1632, 1427, 1250, 1112, 1071 cm^{-1}. HRMS (ESI+, m/z): calcd for $C_{38}H_{48}NaO_2Si_2$ [(M + Na)]$^+$ 615.3085, found 615.3082.

syn-**10**. Colorless oil. Yield: 327 mg, 38% (in two steps). R_f (pentane/EtOAc 10/1) = 0.56. ^{1}H NMR (500 MHz, C_6D_6): δ = 7.79−7.74 (m, 4H), 7.31−7.27 (m, 2H), 7.25−7.08 (m, 9H), 5.03 (s, 1H), 4.84 (s, 1H), 4.04 (t, J = 10.5 Hz, 1H), 3.96 (dd, J = 10.5, 4.0 Hz, 1H), 3.91−3.84 (m, 1H), 2.88 (brs, 1H), 2.23 (dd, J = 10.5, 4.0 Hz, 1H), 2.04 (dd, J = 13.5, 10.0 Hz, 1H), 1.98−1.92 (m, 1H), 1.69−1.58 (m, 1H), 1.50−1.39 (m, 1H), 1.17 (s, 9H), 1.06 (t, J = 7.5 Hz, 3H), 0.14 (s, 3H), 0.11 (s, 3H). ^{13}C NMR (125 MHz, C_6D_6): δ = 146.4, 137.2, 136.0, 135.9, 134.1, 133.7, 133.6, 130.01, 129.99, 129.4, 128.10, 128.07, 128.0, 111.8, 69.3, 65.4, 47.8, 39.4, 30.2, 26.9, 19.4, 10.7, −4.2, −4.8. IR (thin film): 3483, 3071, 2959, 2858, 1631, 1427, 1249, 1112, 1069 cm^{-1}. HRMS (ESI+, m/z): calcd for $C_{32}H_{44}NaO_2Si_2$ [(M + Na)]$^+$ 539.2772, found 539.2761.

anti-**10**. Colorless oil. Yield: 302 mg, 35% (in two steps). R_f (pentane/EtOAc 10/1) = 0.50. ^{1}H NMR (400 MHz, C_6D_6): δ = 7.82−7.71 (m, 4H), 7.33−7.28 (m, 2H), 7.26−7.09 (m, 9H), 4.99 (s, 1H), 4.79 (s, 1H), 4.01 (t, J = 10.4 Hz, 1H), 3.97 (dd, J = 10.0, 4.8 Hz, 1H), 3.85−3.77 (m, 1H), 3.16 (d, J = 2.4 Hz, 1H), 2.56 (dd, J = 10.0, 4.8 Hz, 1H), 2.17 (dd, J = 13.2, 3.2 Hz, 1H), 1.94 (dd, J = 13.2, 9.6 Hz, 1H), 1.63−1.42 (m, 2H), 1.17 (s, 9H), 1.01 (t, J = 7.6 Hz, 3H), 0.15 (s, 3H), 0.13 (s, 3H). ^{13}C NMR (100 MHz, C_6D_6): δ = 148.1, 137.2, 136.02, 135.96, 134.2, 133.5, 133.4, 130.03, 129.97, 129.4, 128.1, 128.0, 127.9, 110.5, 74.7, 66.0, 47.7, 41.4, 30.7, 26.9, 19.3, 10.4, −3.9, −4.9. IR (thin film): 3466, 3071, 2959, 2859, 1631, 1428, 1250, 1186, 1112, 1064 cm^{-1}. HRMS (ESI+, m/z): calcd for $C_{32}H_{44}NaO_2Si_2$ [(M + Na)]$^+$ 539.2772, found 539.2772.

syn-**11**. Colorless oil. Yield: 314 mg, 33% (in two steps). R_f (pentane/EtOAc 10/1) = 0.58. ^{1}H NMR (500 MHz, C_6D_6): δ = 7.80−7.75 (m, 4H), 7.33−7.29 (m, 2H), 7.25−7.19 (m, 6H), 7.18−7.09 (m, 3H), 5.06 (s, 1H), 4.86 (s, 1H), 4.05 (t, J = 10.5 Hz, 1H), 3.97 (dd, J = 10.5, 4.0 Hz, 1H), 3.79−3.73 (m, 1H), 2.83 (d, J = 2.0 Hz, 1H), 2.24 (dd, J = 10.5, 4.0 Hz, 1H), 2.19−2.12 (m, 1H), 2.09 (dd, J = 13.0, 10.5 Hz, 1H), 1.99 (d, J = 12.5 Hz, 1H), 1.82−1.60 (m, 4H), 1.48−1.39 (m, 1H), 1.30−1.09 (m, 14H), 0.16 (s, 3H), 0.13 (s, 3H). ^{13}C NMR (125 MHz, C_6D_6): δ = 146.7, 137.2, 136.05, 135.95, 134.1, 133.70, 133.67, 130.01, 129.99, 129.4, 128.12, 128.08, 128.0, 111.8, 71.6, 65.4, 45.2, 43.8, 39.1, 29.6, 29.1, 27.1, 27.0, 26.8, 26.7, 19.4, −4.2, −4.7. IR (thin film): 3488, 3071, 2929, 2856, 1632, 1428, 1250, 1112, 1064 cm^{-1}. HRMS (ESI+, m/z): calcd for $C_{36}H_{50}NaO_2Si_2$ [(M + Na)]$^+$ 593.3242, found 593.3234.

anti-**11**. Colorless oil. Yield: 286 mg, 30% (in two steps). R_f (pentane/EtOAc 10/1) = 0.57. ^{1}H NMR (500 MHz, C_6D_6): δ = 7.83−7.77 (m, 2H), 7.76−7.71 (m, 2H), 7.33−7.29 (m, 2H), 7.26−7.08 (m, 9H), 5.04 (s, 1H), 4.82 (s, 1H), 4.03 (t, J = 10.5 Hz, 1H), 3.99 (dd, J = 10.5, 5.0 Hz, 1H), 3.74−3.69 (m, 1H), 3.28 (d, J = 2.5 Hz, 1H), 2.62 (dd, J = 10.5, 4.5 Hz, 1H), 2.25 (dd, J = 13.0, 2.0 Hz, 1H), 2.09−2.03 (m, 1H), 1.99 (dd, J = 13.0, 10.0 Hz, 1H), 1.81−1.67 (m, 3H), 1.66−1.60 (m, 1H), 1.47−1.38 (m, 1H), 1.26−1.10 (m, 14H), 0.16 (s, 3H), 0.14 (s, 3H). ^{13}C NMR (125 MHz, C_6D_6): δ =

dx.doi.org/10.1021/jo301953h | J. Org. Chem. 2013, 78, 104−115

148.7, 137.2, 136.06, 135.98, 134.2, 133.5, 133.4, 130.05, 129.98, 129.4, 128.1, 128.1, 128.0, 110.6, 77.6, 66.0, 44.8, 44.2, 41.6, 29.6, 28.5, 27.1, 26.9, 26.8, 26.7, 19.3, −3.9, −4.9. IR (thin film): 3465, 3071, 2928, 2856, 1630, 1427, 1249, 1187, 1112, 1064 cm^{-1}. HRMS (ESI+, *m*/*z*): calcd for $C_{36}H_{50}NaO_2Si_2$ $[(M + Na)]^+$ 593.3242, found 593.3228.

syn-**12**. Colorless oil. Yield: 377 mg, 40% (in two steps). R_f (pentane/EtOAc 10/1) = 0.60. ^1H NMR (500 MHz, C_6D_6): δ = 7.82−7.77 (m, 4H), 7.51−7.47 (m, 2H), 7.30−7.08 (m, 14H), 5.12−5.07 (m, 1H), 5.06 (s, 1H), 4.88 (s, 1H), 4.09 (t, *J* = 10.5 Hz, 1H), 4.01 (dd, *J* = 10.5, 4.5 Hz, 1H), 3.30 (d, *J* = 2.0 Hz, 1H), 2.38−2.22 (m, 3H), 1.18 (s, 9H), 0.12 (s, 3H), 0.10 (s, 3H). ^{13}C NMR (125 MHz, C_6D_6): δ = 145.9, 145.0, 137.1, 136.06, 135.98, 134.1, 133.64, 133.61, 130.07, 130.05, 129.5, 128.4, 128.13, 128.11, 128.0, 127.1, 126.1, 112.6, 70.5, 65.2, 50.5, 39.3, 27.0, 19.4, −4.2, −4.6. IR (thin film): 3467, 3071, 2956, 2859, 1632, 1250, 1195, 1112, 1061 cm^{-1}. HRMS (ESI+, *m*/*z*): calcd for $C_{36}H_{44}NaO_2Si_2$ $[(M + Na)]^+$ 587.2772, found 587.2758.

anti-**12**. Colorless oil. Yield: 348 mg, 37% (in two steps). R_f (pentane/EtOAc 10/1) = 0.50. ^1H NMR (500 MHz, C_6D_6): δ = 7.82−7.78 (m, 2H), 7.77−7.73 (m, 2H), 7.50−7.46 (m, 2H), 7.30−7.07 (m, 14H), 5.08−5.02 (m, 2H), 4.83 (s, 1H), 4.04 (t, *J* = 10.5 Hz, 1H), 4.01 (dd, *J* = 10.5, 5.0 Hz, 1H), 3.66 (d, *J* = 2.5 Hz, 1H), 2.61 (dd, *J* = 10.5, 4.5 Hz, 1H), 2.51 (dd, *J* = 13.5, 3.0 Hz, 1H), 2.28 (dd, *J* = 14.0, 10.0 Hz, 1H), 1.18 (s, 9H), 0.12 (s, 3H), 0.11 (s, 3H). ^{13}C NMR (125 MHz, C_6D_6): δ = 147.5, 145.3, 137.0, 136.04, 136.00, 134.2, 133.5, 133.4, 130.1, 130.0, 129.4, 128.4, 128.1, 128.1, 128.0, 127.2, 126.0, 111.2, 75.8, 66.1, 50.5, 41.5, 26.9, 19.3, −3.9, −5.0. IR (thin film): 3443, 3070, 2956, 2858, 1630, 1427, 1250, 1194, 1112, 1065 cm^{-1}. HRMS (ESI+, *m*/*z*): calcd for $C_{36}H_{44}NaO_2Si_2$ $[(M + Na)]^+$ 587.2772, found 587.2765.

13a and **13b**. A mixture of **8** (50.0 mg, 0.167 mmol), zinc powder (12.0 mg, 0.184 mmol), and benzaldehyde (19.7 mg, 0.184 mmol) in THF−satd NH_4Cl aq (1 mL−0.1 mL) was stirred for 2 h. After dilution with Et_2O, the separated aqueous phase was extracted with Et_2O, and the combined organic solutions were dried with Na_2SO_4 and concentrated. The residual oil was purified by column chromatography (silica gel, 0%→20% EtOAc/pentane) to give **13a** (21.8 mg, 40% yield) and **13b** (19.1 mg, 35% yield), respectively.

13a. Colorless oil. R_f (pentane/EtOAc 5/1) = 0.45. ^1H NMR (500 MHz, C_6D_6): δ = 7.39−7.34 (m, 4H), 7.22−7.14 (m, 5H), 7.12−7.07 (m, 1H), 5.02 (s, 1H), 4.93 (dd, *J* = 10.5, 3.0 Hz, 1H), 4.77 (s, 1H), 3.70−3.58 (m, 3H), 2.50 (brs, 1H), 2.29 (dd, *J* = 14.0, 11.0 Hz, 1H), 2.18−2.09 (m, 2H), 0.16 (s, 6H). ^{13}C NMR (125 MHz, C_6D_6): δ = 145.4, 145.1, 137.3, 134.2, 129.5, 128.5, 128.1, 127.2, 126.0, 112.9, 70.6, 63.2, 50.1, 38.8, −4.2, −4.8. IR (thin film): 3351, 3069, 2954, 1633, 1427, 1249, 1112, 1058 cm^{-1}. HRMS (ESI+, *m*/*z*): calcd for $C_{20}H_{26}NaO_2Si$ $[(M + Na)]^+$ 349.1594, found 349.1601.

13b. Colorless oil. R_f (pentane/EtOAc 5/1) = 0.44. ^1H NMR (500 MHz, C_6D_6): δ = 7.40−7.34 (m, 4H), 7.21−7.13 (m, 5H), 7.12−7.06 (m, 1H), 4.97 (s, 1H), 4.84 (dd, *J* = 9.5, 3.5 Hz, 1H), 4.75 (s, 1H), 3.68 (br, s), 3.63 (d, *J* = 8.5 Hz, 2H), 2.39 (dd, *J* = 13.0, 3.5 Hz, 1H), 2.36 (d, *J* = 8.5 Hz, 1H), 2.16 (dd, *J* = 13.0, 9.5 Hz, 1H), 2.03 (brs, 1H), 0.16 (s, 3H), 0.15 (s, 3H). ^{13}C NMR (125 MHz, C_6D_6): δ = 147.4, 145.3, 137.2, 134.3, 129.5, 128.5, 128.1, 127.3, 126.0, 110.9, 76.6, 64.0, 50.2, 41.7, −4.0, −5.1. IR (thin film): 3338, 3069, 2954, 1631, 1427, 1249, 1112, 1060 cm^{-1}. HRMS (ESI+, *m*/*z*): calcd for $C_{20}H_{26}NaO_2Si$ $[(M + Na)]^+$ 349.1594, found 349.1604.

14a. To a solution of **13a** (16.0 mg, 0.0491 mmol) and Et_3N (50.0 mg, 0.491 mmol) in CH_2Cl_2 (0.5 mL) was added TsCl (14.0 mg, 0.0737 mmol) at rt. The mixture was stirred at rt for 17 h, and water was added. The separated aqueous phase was extracted with CH_2Cl_2, and the combined organic solutions were washed with brine, dried with Na_2SO_4, and concentrated in vacuo. The residue was purified by chromatography (silica gel, 10% CH_2Cl_2/pentane) to give **14a** (7.1 mg, 47% yield) as a colorless oil. R_f (pentane/CH_2Cl_2 10/1) = 0.49. ^1H NMR (500 MHz, $CDCl_3$): δ = 7.61−7.56 (m, 2H), 7.37−7.23 (m, 8H), 4.94−4.91 (m, 1H), 4.86−4.83 (m, 1H), 4.81 (dd, *J* = 10.0, 5.5 Hz, 1H), 4.52−4.46 (m, 1H), 2.92 (dd, *J* = 15.5, 5.5 Hz, 1H), 2.50−2.42 (m, 1H), 1.34 (dd, *J* = 15.0, 4.0 Hz, 1H), 1.24 (dd, *J* = 15.0, 9.5 Hz, 1H), 0.40 (s, 3H), 0.39 (s, 3H). ^{13}C NMR (125 MHz, $CDCl_3$): δ = 154.4, 142.3, 139.8, 133.8, 128.8, 128.3, 127.8, 127.3, 125.8, 103.9, 79.4, 79.2, 41.7, 22.9, −1.6, −2.0. IR (thin film): 3069, 2955, 2922, 2853, 1665, 1427, 1247, 1112, 1086 cm^{-1}. HRMS (ESI+, *m*/*z*): calcd for $C_{20}H_{24}NaOSi$ $[(M + Na)]^+$ 331.1489, found 331.1486.

14b. To a solution of **13b** (8.6 mg, 0.0263 mmol) and Et_3N (27.0 mg, 0.263 mmol) in CH_2Cl_2 (0.5 mL) was added TsCl (7.5 mg, 0.0395 mmol) at rt. The mixture was stirred at rt for 17 h, and water was added. The separated aqueous phase was extracted with CH_2Cl_2, and the combined organic solutions were washed with brine, dried with Na_2SO_4, and concentrated in vacuo. The residue was purified by chromatography (silica gel, 10% CH_2Cl_2/pentane) to give **14b** (5.6 mg, 69% yield) as a colorless oil. R_f (pentane/CH_2Cl_2 10/1) = 0.45. ^1H NMR (500 MHz, $CDCl_3$): δ = 7.60−7.56 (m, 2H), 7.37−7.22 (m, 8H), 5.04 (t, *J* = 7.0 Hz, 1H), 4.92 (dd, *J* = 4.0, 2.0 Hz, 1H), 4.83 (dd, *J* = 4.0, 2.0 Hz, 1H), 4.70−4.65 (m, 1H), 3.04−2.97 (m, 1H), 2.64−2.58 (m, 1H), 1.27 (dd, *J* = 15.0, 9.5 Hz, 1H), 1.23 (dd, *J* = 15.0, 5.0 Hz, 1H), 0.41 (s, 3H), 0.38 (s, 3H). ^{13}C NMR (125 MHz, $CDCl_3$): δ = 154.1, 143.0, 139.7, 133.8, 128.9, 128.3, 127.8, 127.2, 125.8, 104.3, 78.4, 77.6, 40.6, 23.4, −1.6, −2.2. IR (thin film): 3068, 2954, 2922, 2853, 1667, 1427, 1246, 1112, 1056 cm^{-1}. HRMS (ESI+, *m*/*z*): calcd for $C_{20}H_{24}NaOSi$ $[(M + Na)]^+$ 331.1489, found 331.1491.

syn-**12**. To a solution of **14a** (8.5 mg, 0.0261 mmol) in DMF (0.5 mL) were added TBDPSCl (8.9 mg, 0.0313 mmol) and imidazole (4.4 mg, 0.0653 mmol). The mixture was stirred at rt for 1 h and diluted with water and Et_2O. The separated aqueous phase was extracted with Et_2O, and the combined organic solutions were washed with brine, dried with Na_2SO_4, and concentrated in vacuo. The residue was purified by chromatography (silica gel, 0%→2% EtOAc/pentane) to give *syn*-**12** (12.0 mg, 82% yield) as a colorless oil.

anti-**12**. To a solution of **14b** (7.0 mg, 0.0215 mmol) in DMF (0.5 mL) was added TBDPSCl (9.2 mg, 0.0258 mmol) and imidazole (3.7 mg, 0.0538 mmol). The mixture was stirred at rt for 1 h and diluted with water and Et_2O. The separated aqueous phase was extracted with Et_2O, and the combined organic solutions were washed with brine, dried with Na_2SO_4, and concentrated in vacuo. The residue was purified by chromatography (silica gel, 0%→2% EtOAc/pentane) to give *anti*-**12** (9.7 mg, 80% yield) as a colorless oil.

General Procedure for TMSOTf-Promoted Cyclization of *β*-Hydroxy Allylsilanes. To a solution of *β*-hydroxy allylsilane (0.030 mmol) in Et_2O (1.0 mL) was added aldehyde (0.060 mmol), and the mixture was cooled to −78 °C. TMSOTf (8.1 *μ*L, 0.045 mmol) was added, and the mixture was stirred until the starting material completely disappeared (monitored by TLC). The reaction was quenched with satd $NaHCO_3$ aq, and then aqueous layer was extracted with Et_2O. The combined organic layer was dried with Na_2SO_4 and concentrated in vacuo. The residue was purified by chromatography with EtOAc−pentane to give cyclized product.

15a. Colorless oil. Yield: 14.3 mg, 96% (from *syn*-**9**); 14.0 mg, 94%, 82:18 dr (from *anti*-**10**). R_f (pentane/EtOAc 10/1) = 0.88. ^1H NMR (500 MHz, $CDCl_3$): δ = 7.69−7.65 (m, 4H), 7.44−7.33 (m, 6H), 7.30−7.25 (m, 2H), 7.21−7.15 (m, 3H), 5.37 (t, *J* = 6.5 Hz, 1H), 4.23 (dd, *J* = 12.5, 6.5 Hz, 1H), 4.19 (dd, *J* = 12.5, 6.5 Hz, 1H), 3.21−3.14 (m, 1H), 2.96−2.89 (m, 1H), 2.80 (ddd, *J* = 13.5, 9.5, 5.5 Hz, 1H), 2.69 (dt, *J* = 13.5, 9.0 Hz, 1H), 2.21 (d, *J* = 13.5 Hz, 1H), 2.05 (d, *J* = 13.0 Hz, 1H), 1.94 (t, *J* = 12.0 Hz, 1H), 1.90−1.81 (m, 1H), 1.74−1.65 (m, 1H), 1.56−1.46 (m, 2H), 1.44−1.33 (m, 1H), 1.03 (s, 9H), 0.94 (t, *J* = 7.0 Hz, 3H). ^{13}C NMR (125 MHz, $CDCl_3$): δ = 142.4, 137.0, 135.71, 135.69, 134.00, 133.96, 129.6, 128.6, 128.4, 127.70, 127.68, 125.8, 122.6, 78.9, 77.0, 60.1, 42.2, 37.9, 34.9, 31.8, 29.4, 26.9, 19.2, 10.4. IR (thin film): 3070, 3027, 2931, 2857, 1671, 1603, 1589, 1428, 1111, 1069 cm^{-1}. HRMS (ESI+, *m*/*z*): calcd for $C_{33}H_{42}NaO_2Si$ $[(M + Na)]^+$ 521.2846, found 521.2834.

15b. Colorless oil. Yield: 15.4 mg, 93% (from *syn*-**9**); 15.7 mg, 95%, 79:21 dr (from *anti*-**11**). R_f (pentane/EtOAc 10/1) = 0.89. ^1H NMR (500 MHz, $CDCl_3$): δ = 7.70−7.65 (m, 4H), 7.44−7.33 (m, 6H), 7.31−7.24 (m, 2H), 7.21−7.16 (m, 3H), 5.37 (t, *J* = 6.5 Hz, 1H), 4.22 (dd, *J* = 12.5, 6.5 Hz, 1H), 4.19 (dd, *J* = 12.5, 6.5 Hz, 1H), 3.17−3.10 (m, 1H), 2.83−2.65 (m, 3H), 2.27 (d, *J* = 13.5 Hz, 1H), 2.03 (d, *J* = 13.0 Hz, 2H), 1.96−1.80 (m, 2H), 1.78−1.61 (m, 4H), 1.60−1.46 (m,

dx.doi.org/10.1021/jo301953h | *J. Org. Chem.* 2013, 78, 104−115

2H), 1.26−1.08 (m, 4H), 1.03 (s, 9H), 1.02−0.85 (m, 2H). ^{13}C NMR (125 MHz, $CDCl_3$): δ = 142.4, 137.3, 135.7, 134.0, 129.6, 128.7, 128.3, 127.7, 125.7, 122.7, 81.7, 76.8, 60.0, 43.3, 42.4, 38.0, 32.2, 31.8, 29.3, 29.0, 26.9, 26.7, 26.2, 26.1, 19.2. IR (thin film): 3070, 3026, 2929, 2855, 1671, 1603, 1589, 1428, 1111, 1059 cm^{-1}. HRMS (ESI+, m/z): calcd for $C_{37}H_{48}NaO_2Si$ [(M + Na)]$^+$ 575.3316, found 575.3316.

15c. Colorless oil. Yield: 14.2 mg, 90% (from *syn*-**9**). R_f (pentane/EtOAc 10/1) = 0.90. ^{1}H NMR (500 MHz, $CDCl_3$): δ = 7.71−7.65 (m, 4H), 7.44−7.33 (m, 6H), 7.31−7.25 (m, 2H), 7.21−7.16 (m, 3H), 5.38 (t, J = 6.5 Hz, 1H), 4.22 (dd, J = 12.5, 6.5 Hz, 1H), 4.19 (dd, J = 12.5, 6.5 Hz, 1H), 3.19−3.12 (m, 1H), 2.80 (ddd, J = 14.0, 9.0, 5.0 Hz, 1H), 2.72−2.64 (m, 2H), 2.20 (d, J = 13.0 Hz, 1H), 2.05 (d, J = 13.0 Hz, 1H), 1.92−1.77 (m, 2H), 1.73−1.64 (m, 1H), 1.52 (t, J = 12.5 Hz, 1H), 1.03 (s, 9H), 0.86 (s, 9H). ^{13}C NMR (125 MHz, $CDCl_3$): δ = 142.6, 137.9, 135.7, 134.0, 129.6, 128.7, 128.3, 127.7, 125.7, 122.5, 84.7, 76.8, 60.0, 42.4, 38.1, 34.4, 31.8, 29.1, 26.9, 26.1, 19.2. IR (thin film): 3070, 2953, 2858, 1671, 1608, 1589, 1428, 1361, 1111, 1062 cm^{-1}. HRMS (ESI+, m/z): calcd for $C_{35}H_{46}NaO_2Si$ [(M + Na)]$^+$ 549.3159, found 549.3154.

15d. Colorless oil. Yield: 15.1 mg, 92% (from *syn*-**9**); 12.9 mg, 79%, 92:8 dr (from *anti*-**12**). R_f (pentane/EtOAc 10/1) = 0.88. ^{1}H NMR (500 MHz, $CDCl_3$): δ = 7.70−7.65 (m, 4H), 7.42−7.14 (m, 16H), 5.48 (t, J = 6.5 Hz, 1H), 4.28 (dd, J = 12.5, 6.5 Hz, 1H), 4.22 (dd, J = 12.5, 6.5 Hz, 1H), 4.11 (dd, J = 11.5, 2.0 Hz, 1H), 3.44−3.38 (m, 1H), 2.82 (ddd, J = 13.5, 9.0, 5.5 Hz, 1H), 2.77−2.69 (m, 1H), 2.48 (d, J = 13.5 Hz, 1H), 2.16 (d, J = 13.0 Hz, 1H), 2.08 (t, J = 12.0 Hz, 1H), 2.00−1.91 (m, 1H), 1.89−1.76 (m, 2H), 1.04 (s, 9H). ^{13}C NMR (125 MHz, $CDCl_3$): δ = 142.6, 142.3, 136.5, 135.71, 135.67, 133.93, 133.85, 129.7, 128.6, 128.4, 128.3, 127.7, 127.5, 125.9, 125.8, 123.4, 79.0, 77.5, 60.1, 41.7, 37.9, 36.8, 31.7, 26.9, 19.2. IR (thin film): 3069, 3027, 2931, 2857, 1671, 1603, 1428, 1111, 1058 cm^{-1}. HRMS (ESI+, m/z): calcd for $C_{37}H_{42}NaO_2Si$ [(M + Na)]$^+$ 569.2846, found 569.2839.

15e. Colorless oil. Yield: 16.3 mg, 95% (from *syn*-**9**). R_f (pentane/EtOAc 10/1) = 0.90. ^{1}H NMR (500 MHz, $CDCl_3$): δ = 7.71−7.66 (m, 4H), 7.44−7.16 (m, 16H), 6.53 (d, J = 16.0 Hz, 1H), 6.18 (dd, J = 16.0, 5.5 Hz, 1H), 5.45 (t, J = 6.5 Hz, 1H), 4.28 (dd, J = 12.5, 6.5 Hz, 1H), 4.27 (dd, J = 12.5, 6.5 Hz, 1H), 4.22 (dd, J = 12.5, 6.0 Hz, 1H), 3.76−3.70 (m, 1H), 3.36−3.29 (m, 1H), 2.82 (ddd, J = 13.5, 9.0, 5.5 Hz, 1H), 2.77−2.68 (m, 1H), 2.35 (d, J = 13.5 Hz, 1H), 2.13 (d, J = 13.0 Hz, 1H), 2.05−1.89 (m, 2H), 1.82−1.71 (m, 2H), 1.04 (s, 9H). ^{13}C NMR (125 MHz, $CDCl_3$): δ = 142.2, 136.9, 136.1, 135.73, 135.70, 133.94, 133.86, 130.3, 130.1, 129.7, 128.6, 128.4, 127.74, 127.72, 127.65, 126.5, 125.8, 123.4, 77.7, 77.3, 60.1, 41.7, 37.8, 35.2, 31.8, 26.9, 19.2. IR (thin film): 3069, 3026, 2931, 2857, 1672, 1601, 1589, 1428, 1111, 1057 cm^{-1}. HRMS (ESI+, m/z): calcd for $C_{39}H_{44}NaO_2Si$ [(M + Na)]$^+$ 595.3003, found 595.2994.

16a. Colorless oil. Yield: 14.3 mg, 96% (from *syn*-**10**); 14.2 mg, 95%, 84:16 dr (from *anti*-**9**). R_f (pentane/EtOAc 10/1) = 0.90. ^{1}H NMR (500 MHz, $CDCl_3$): δ = 7.69−7.64 (m, 4H), 7.43−7.30 (m, 6H), 7.29−7.24 (m, 2H), 7.19−7.14 (m, 3H), 5.39 (t, J = 6.5 Hz, 1H), 4.21 (dd, J = 12.5, 6.5 Hz, 1H), 4.17 (dd, J = 12.5, 6.5 Hz), 3.15−3.08 (m, 1H), 3.06−2.99 (m, 1H), 2.76 (ddd, J = 13.5, 9.5, 5.5 Hz, 1H), 2.65 (dt, J = 14.0, 8.5 Hz, 1H), 2.15 (d, J = 13.5 Hz, 1H), 2.11 (d, J = 13.0 Hz, 1H), 1.90 (t, J = 12.5 Hz, 1H), 1.85−1.75 (m, 1H), 1.64−1.43 (m, 4H), 1.03 (s, 9H), 1.00 (t, J = 7.5 Hz, 3H). ^{13}C NMR (125 MHz, $CDCl_3$): δ = 142.3, 136.9, 135.7, 134.0, 129.7, 128.6, 128.4, 127.69, 127.67, 125.8, 122.6, 79.8, 76.2, 60.1, 41.8, 38.0, 35.2, 31.8, 29.4, 26.9, 19.2, 10.3. IR (thin film): 3070, 3026, 2931, 2857, 1670, 1603, 1589, 1428, 1111 cm^{-1}. HRMS (ESI+, m/z): calcd for $C_{33}H_{42}NaO_2Si$ [(M + Na)]$^+$ 521.2846, found 521.2844.

16b. Colorless oil. Yield: 15.7 mg, 95% (from *syn*-**11**); 15.7 mg, 95%, 84:16 dr (from *anti*-**9**). R_f (pentane/EtOAc 10/1) = 0.89. ^{1}H NMR (500 MHz, $CDCl_3$): δ = 7.69−7.64 (m, 4H), 7.43−7.24 (m, 8H), 7.20−7.15 (m, 3H), 5.39 (t, J = 6.5 Hz, 1H), 4.20 (dd, J = 12.5, 7.0 Hz, 1H), 4.17 (dd, J = 12.5, 6.5 Hz, 1H), 3.02−2.95 (m, 1H), 2.92 (ddd, J = 11.0, 7.5, 2.0 Hz, 1H), 2.76 (ddd, J = 14.0, 8.5, 4.5 Hz, 1H), 2.66 (dt, J = 14.0, 8.0 Hz, 1H), 2.19−2.06 (m, 3H), 1.89 (t, J = 11.5 Hz, 1H), 1.84−1.63 (m, 5H), 1.62−1.49 (m, 2H), 1.45−1.34 (m, 1H), 1.32−1.12 (m, 3H), 1.08−0.96 (m, 11H). ^{13}C NMR (125 MHz, $CDCl_3$): δ = 142.4, 137.2, 135.7, 134.0, 129.6, 128.7, 128.4, 127.68, 127.66, 125.7, 122.7, 82.5, 76.0, 60.1, 43.3, 39.4, 38.1, 35.4, 31.8, 29.5, 28.9, 26.9, 26.7, 26.3, 26.1, 19.2. IR (thin film): 3070, 3026, 2928, 2855, 1671, 1603, 1589, 1428, 1111, 1058 cm^{-1}. HRMS (ESI+, m/z): calcd for $C_{37}H_{48}NaO_2Si$ [(M + Na)]$^+$ 575.3316, found 575.3303.

16c. Colorless oil. Yield: 12.6 mg, 80%, 92:8 dr (from *anti*-**9**). R_f (pentane/EtOAc 10/1) = 0.90. ^{1}H NMR (500 MHz, $CDCl_3$): δ = 7.70−7.64 (m, 4H), 7.43−7.30 (m, 6H), 7.29−7.24 (m, 2H), 7.21−7.14 (m, 3H), 5.39 (t, J = 6.5 Hz, 1H), 4.23−4.14 (m, 2H), 3.03−2.96 (m, 1H), 2.85 (dd, J = 11.5, 2.0 Hz, 1H), 2.76 (ddd, J = 14.0, 9.0, 5.0 Hz, 1H), 2.64 (dt, J = 14.0, 8.5 Hz, 1H), 2.11 (d, J = 13.5 Hz, 1H), 2.06 (d, J = 13.5 Hz, 1H), 1.94 (t, J = 12.0 Hz, 1H), 1.80−1.71 (m, 1H), 1.62−1.54 (m, 1H), 1.49 (t, J = 12.0 Hz, 1H), 1.02 (s, 9H), 0.94 (s, 9H). ^{13}C NMR (125 MHz, $CDCl_3$): δ = 142.6, 137.8, 135.7, 134.01, 134.00, 129.6, 128.6, 128.3, 127.69, 127.66, 125.7, 122.6, 85.6, 76.0, 60.2, 38.2, 36.3, 35.3, 34.3, 31.8, 26.9, 26.1, 19.2. IR (thin film): 3070, 2954, 2858, 1671, 1603, 1589, 1428, 1361, 1111, 1061 cm^{-1}. HRMS (ESI+, m/z): calcd for $C_{35}H_{46}NaO_2Si$ [(M + Na)]$^+$ 549.3159, found 549.3148.

16d. Colorless oil. Yield: 15.2 mg, 93% (from *syn*-**12**); 14.6 mg, 89% (from *anti*-**9**). R_f (pentane/EtOAc 10/1) = 0.88. ^{1}H NMR (500 MHz, $CDCl_3$): δ = 7.71−7.66 (m, 4H), 7.45−7.33 (m, 10H), 7.35−7.23 (m, 3H), 7.20−7.14 (m, 3H), 5.49 (t, J = 6.5 Hz, 1H), 4.30 (dd, J = 11.5, 2.5 Hz, 1H), 4.28−4.19 (m, 2H), 3.28−3.20 (m, 1H), 2.78 (ddd, J = 13.5, 9.0, 5.0 Hz, 1H), 2.68 (ddd, J = 13.5, 9.0, 7.0 Hz, 1H), 2.36 (d, J = 13.5 Hz, 1H), 2.28−2.17 (m, 2H), 1.94−1.84 (m, 1H), 1.75−1.63 (m, 2H), 1.05 (s, 9H). ^{13}C NMR (125 MHz, $CDCl_3$): δ = 142.7, 142.3, 136.5, 135.71, 135.70, 134.0, 133.9, 129.7, 128.6, 128.4, 127.73, 127.71, 127.4, 125.82, 125.79, 123.3, 79.8, 76.7, 60.1, 43.9, 38.0, 34.8, 31.7, 26.9, 19.2. IR (thin film): 3069, 3027, 2930, 2856, 1673, 1603, 1589, 1427, 1111, 1056 cm^{-1}. HRMS (ESI+, m/z): calcd for $C_{37}H_{42}NaO_2Si$ [(M + Na)]$^+$ 569.2846, found 569.2838.

16e. Colorless oil. Yield: 16.1 mg, 94%, 94:6 dr (from *anti*-**9**). R_f (pentane/EtOAc 10/1) = 0.90. ^{1}H NMR (500 MHz, $CDCl_3$): δ = 7.71−7.66 (m, 4H), 7.45−7.14 (m, 16H), 6.63 (d, J = 16.0 Hz, 1H), 6.26 (dd, J = 16.0, 6.0 Hz, 1H), 5.46 (t, J = 6.5 Hz, 1H), 4.27−4.17 (m, 2H), 3.95−3.89 (m, 1H), 3.19−3.12 (m, 1H), 2.77 (ddd, J = 13.5, 9.0, 5.0 Hz, 1H), 2.67 (ddd, J = 14.0, 9.0, 7.5 Hz, 1H), 2.26−2.10 (m, 3H), 1.92−1.82 (m, 1H), 1.71−1.64 (m, 1H), 1.61 (t, J = 12.5 Hz, 1H), 1.04 (s, 9H). ^{13}C NMR (125 MHz, $CDCl_3$): δ = 142.2, 136.9, 136.1, 135.7, 133.93, 133.89, 130.3, 130.2, 129.7, 128.6, 128.4, 127.72, 127.66, 126.6, 125.8, 123.4, 78.6, 76.5, 60.1, 42.1, 37.9, 34.8, 31.8, 26.9, 19.2. IR (thin film): 3069, 3026, 2931, 2857, 1672, 1601, 1589, 1428, 1111, 1056 cm^{-1}. HRMS (ESI+, m/z): calcd for $C_{39}H_{44}NaO_2Si$ [(M + Na)]$^+$ 595.3003, found 595.3001.

Computational Methods. All structures were optimized with the B3LYP/6-31G(d) model chemistry[33,34] using Gaussian 09.[35] Frequency calculations were used to characterize stationary points as minima or transition-state structures along with intrinsic reaction coordinate (IRC) calculations[36] to connect transition-state structures to their respective minima. Single-point energies were calculated for the B3LYP/6-31G(d) geometries at multiple model chemistries including CAM-B3LYP/6-31+G(d,p),[37] M06-2X/6-31+G(d,p),[38] and B3LYP/6-31+G(d,p). Single-point solvent calculations were carried out using the SMD solvent model[39] with diethyl ether. Figures were generated using Ball & Stick.[40] Coordinates for all optimized structures, as well as energies computed with the various methods listed above, can be found in the Supporting Information.

■ ASSOCIATED CONTENT

Supporting Information

^{1}H and ^{13}C NMR spectra of all new compounds. Additional details on computations, including coordinate and energies for computed structures. This material is available free of charge via the Internet at http://pubs.acs.org.

■ AUTHOR INFORMATION

Corresponding Author

*Email: djtantillo@ucdavis.edu; wenderp@stanford.edu.

Notes

The authors declare no competing financial interest.

■ ACKNOWLEDGMENTS

This research was supported by the National Institutes of Health (P.A.W., CA31845) and the National Science Foundation (D.J.T., CHE-0957416 and supercomputer resources through CHE030089).

■ DEDICATION

This article is dedicated to the memory of Professor Robert E. Ireland whose inspiration continues.

■ REFERENCES

(1) Pettit, G. R.; Herald, C. L.; Doubek, D. L.; Herald, D. L.; Arnold, E.; Clardy, J. *J. Am. Chem. Soc.* **1982**, *104*, 6846−6848.

(2) For reviews, see: (a) Wender, P. A.; Loy, B. A.; Schrier, A. J. *Isr. J. Chem.* **2011**, *51*, 453−472. (b) Wender, P. A.; Baryza, J. L.; Hilinski, M. K.; Horan, J. C.; Kan, C.; Verma, V. A. Beyond Natural Products: Synthetic Analogues of Bryostatin 1. In *Drug Discovery Research*; Huang, Z., Ed.; Wiley: Hoboken, 2007; pp 127−162. (c) Pettit, G. R.; Herald, C. L.; Hogan, F. In *Anticancer Drug Development*; Baguley, B. C., Kerr, D. J., Eds.; Academic Press: San Diego, 2002; pp 203−235. (d) Kortmansky, J.; Schwartz, G. K. *Cancer Invest.* **2003**, *21*, 924−936. (e) Hale, K. J.; Hummersone, M. G.; Manaviazar, S.; Frigerio, M. *Nat. Prod. Rep.* **2002**, *19*, 413−453. (f) Hale, K. J.; Manaviazar, S. *Chem. Asian J.* **2010**, *5*, 704−754.

(3) (a) Nelson, T. J.; Alkon, D. L. *Trends Biochem. Sci.* **2009**, *34*, 136−145. (b) Sun, M.-K.; Alkon, D. L. *Arch. Pharm.* **2009**, *342*, 689−698. (c) Khan, T. K.; Nelson, T. J.; Verma, V. A.; Wender, P. A.; Alkon, D. L. *Neurobiol. Dis.* **2009**, *34*, 332−339. (d) Sun, M.-K.; Alkon, D. L. *Pharmacol. Ther.* **2010**, *127*, 66−77.

(4) Mehla, R.; Bivalkar-Mehla, S.; Zhang, R.; Handy, I.; Albrecht, H.; Giri, S.; Nagarkatti, P.; Nagarkatti, M.; Chauhan, A. *PLoS One* **2010**, *5*, e11160.

(5) Wender, P. A.; Cribbs, C. M.; Koehler, K. F.; Sharkey, N. A.; Herald, C. L.; Kamano, Y.; Pettit, G. R.; Blumberg, P. M. *Proc. Natl. Acad. Sci. U.S.A.* **1988**, *85*, 7197−7201.

(6) Wender, P. A.; Miller, B. L. *Nature* **2009**, *460*, 197−201.

(7) Wender, P. A.; De Brabander, J.; Harran, P. G.; Jimenez, J.-M.; Koehler, M. F. T.; Lippa, B.; Park, C.-M.; Shiozaki, M. *J. Am. Chem. Soc.* **1998**, *120*, 4534−4535.

(8) Wender, P. A.; Baryza, J. L.; Bennett, C. E.; Bi, C.; Brenner, S. E.; Clarke, M. O.; Horan, J. C.; Kan, C.; Lacote, E.; Lippa, B.; Nell, P. G.; Turner, T. M. *J. Am. Chem. Soc.* **2002**, *124*, 13648−13649.

(9) For total syntheses of natural bryostatins, see: (a) Kageyama, M.; Tamura, T.; Nantz, M. H.; Roberts, J. C.; Somfai, P.; Whritenour, D. C.; Masamune, S. *J. Am. Chem. Soc.* **1990**, *112*, 7407−7408. (b) Evans, D. A.; Carter, P. H.; Carreira, E. M.; Charette, A. B.; Prunet, J. A.; Lautens, M. *J. Am. Chem. Soc.* **1999**, *121*, 7540−7552. (c) Ohmori, K.; Ogawa, Y.; Obitsu, T.; Ishikawa, Y.; Nishiyama, S.; Yamamura, S. *Angew. Chem., Int. Ed.* **2000**, *39*, 2290−2294. (d) Trost, B. M.; Dong, G. *Nature* **2008**, *456*, 485−488. (e) Keck, G. E.; Poudel, Y. B.; Cummins, T. J.; Rudra, A; Covel, J. A. *J. Am. Chem. Soc.* **2011**, *133*, 744−747. (f) Wender, P. A.; Schrier, A. J. *J. Am. Chem. Soc.* **2011**, *133*, 9228−9231. (g) Lu, Y.; Woo, S. K.; Krische, M. J. *J. Am. Chem. Soc.* **2011**, *133*, 13876−13879. For a formal synthesis, see: (h) Manaviazar, S.; Frigerio, M.; Bhatia, G. S.; Hummersone, M. G.; Aliev, A. E.; Hale, K. J. *Org. Lett.* **2006**, *8*, 4477−4480 and references therein.

(10) Wender, P. A.; Verma, V. A.; Paxton, T. J.; Pillow, T. H. *Acc. Chem. Res.* **2008**, *41*, 40−49.

(11) DeChristopher, B. A.; Loy, B. A.; Marsden, M. D.; Schrier, A. J.; Zack, J. A.; Wender, P. A. *Nature Chem.* **2012**, *4*, 705−710.

(12) Stang, S. L.; Lopez-Campistrous, A.; Song, X.; Dower, N. A.; Blumberg, P. M.; Wender, P. A.; Stone, J. C. *Exp. Hematol.* **2009**, *37*, 122−134.

(13) DeChristopher, B. A.; Fan, A. C.; Felsher, D. W.; Wender, P. A. *Oncotarget* **2012**, *3*, 58−66.

(14) Barr, P. M.; Lazarus, H. M.; Cooper, B. W.; Schluchter, M. D.; Panneerselvam, A.; Jacobberger, J. W.; Hsu, J. W.; Janakiraman, N.; Simic, A.; Dowlati, A.; Remick, S. C. *Am. J. Hematol.* **2009**, *84*, 484−487.

(15) Wender, P. A.; De Brabander, J.; Harran, P. G.; Jimenez, J.-M.; Koehler, M. F. T.; Lippa, B.; Park, C.-M.; Siedenbiedel, C.; Pettit, G. R. *Proc. Natl. Acad. Sci. U.S.A.* **1998**, *95*, 6624−6629.

(16) For a review of pyran synthesis, see: Clark, P. A.; Santos, S. *Eur. J. Org. Chem.* **2006**, 2045−2053.

(17) (a) Marko, I. E.; Bayston, D. J. *Tetrahedron Lett.* **1993**, *34*, 6595−6598. (b) Mekhalfia, A.; Marko, I. E.; Adams, H. *Tetrahedron Lett.* **1991**, *32*, 4783−4786. (c) Marko, I. E.; Mekhalfia, A. *Tetrahedron Lett.* **1992**, *33*, 1799−1802. (d) Marko, I. E.; Mekhalfia, A.; Bayston, D. J.; Adams, H. *J. Org. Chem.* **1992**, *57*, 2211−2213.

(18) (a) Keck, G. E.; Covel, J. A.; Schiff, T.; Yu, T. *Org. Lett.* **2002**, *4*, 1189−1192. (b) Keck, G. E.; Truong, A. P. *Org. Lett.* **2005**, *7*, 2149−2152. (c) Keck, G. E.; Truong, A. P. *Org. Lett.* **2005**, *7*, 2153−2156. (d) Keck, G. E.; Welch, D. S.; Poudel, Y. B. *Tetrahedron Lett.* **2006**, *47*, 8267−8270. (e) Keck, G. E.; Kraft, M. B.; Truong, A. P.; Li, W.; Sanchez, C. C.; Kedei, N.; Lewin, N. E.; Blumberg, P. M. *J. Am. Chem. Soc.* **2008**, *130*, 6660−6661. (f) Keck, G. E.; Li, W.; Kraft, M. B.; Kedei, N.; Lewin, N. E.; Blumberg, P. M. *Org. Lett.* **2009**, *11*, 2277−2280.

(19) For recent examples of application of silyl-terminated Prins cyclization to natural product synthesis, see: (a) Gesinski, M. R.; Rychnovsky, S. D. *J. Am. Chem. Soc.* **2011**, *133*, 9727−9729. (b) Zhu, K.; Panek, J. S. *Org. Lett.* **2011**, *13*, 4652−4655. (c) Ghosh, A. K.; Cheng, X. *Org. Lett.* **2011**, *13*, 4108−4111. (d) Wrona, I. E.; Gozman, A.; Taldone, T.; Chiosis, G.; Panek, J. S. *J. Org. Chem.* **2010**, *75*, 2820−2835. (e) Takahashi, K.; Akao, R.; Honda, T. *J. Org. Chem.* **2009**, *74*, 3424−3429. (f) Lowe, J. T.; Panek, J. S. *Org. Lett.* **2008**, *10*, 3813−3816. (g) Qin, H.-L.; Panek, S. J. *Org. Lett.* **2008**, *10*, 2477−2479.

(20) Wender, P. A.; DeChristopher, B. A.; Schrier, A. J. *J. Am. Chem. Soc.* **2008**, *130*, 6658−6659.

(21) For a recent review, see: (a) Crane, E. A.; Scheidt, K. A. *Angew. Chem., Int. Ed.* **2010**, *49*, 8316−8326. For previous work, see: (b) Custar, D. W.; Zabawa, T. P.; Scheidt, K. A. *J. Am. Chem. Soc.* **2008**, *130*, 804−805. (c) Woo, S. K.; Kwon, M. S.; Lee, E. *Angew. Chem., Int. Ed.* **2008**, *47*, 3242−3244. (d) Bahnck, K. B.; Rychnovsky, S. D. *J. Am. Chem. Soc.* **2008**, *130*, 13177−13181. (e) Gesinski, M. R.; Tadpetch, K.; Rychnovsky, S. D. *Org. Lett.* **2009**, *11*, 5342−5345. (f) Custar, D. W.; Zabawa, T. P.; Hines, J.; Crews, C. M.; Scheidt, K. A. *J. Am. Chem. Soc.* **2009**, *131*, 12406−12414. (g) Yadav, J. S.; Krishana, G. G.; Kumar, S. N. *Tetrahedron* **2010**, *66*, 480−487. (h) Woo, S. K.; Lee, E. *J. Am. Chem. Soc.* **2010**, *132*, 4564−4565.

(22) For recent reviews of the Prins reaction, see: (a) Pastor, I. M.; Yus, M. *Curr. Org. Chem.* **2007**, *11*, 925−957. (b) Olier, C.; Kaafarani, M.; Gastaldi, S.; Bertrand, M. P. *Tetrahedron* **2010**, *66*, 413−445.

(23) Trost, B. M.; Machacek, M. R.; Faulk, B. D. *J. Am. Chem. Soc.* **2006**, *128*, 6745−6754.

(24) Tanaka, K.; Ohta, Y.; Fuji, K.; Taga, T. *Tetrahedron Lett.* **1993**, *34*, 4071−4074. It is also used in bryostatin synthesis; see ref 9b,c,e,g.

(25) For a variant involving bis-allylic silanes, see: Lu, J.; Song, Z.; Zhang, Y.; Gan, Z.; Li, H. *Angew. Chem., Int. Ed.* **2012**, *51*, 5367−5370.

(26) For an example of a constrained allyl silane (cyclohexenylsilane) in a Prins process, see: Pham, M.; Allatabakhsh, A.; Minehan, T. G. *J. Org. Chem.* **2008**, *73*, 741−744.

(27) For an excellent review, see: Masse, C. E.; Panek., J. S. *Chem. Rev.* **1995**, *95*, 1293−1316.

(28) Fukuda, K.; Miyashita, M.; Tanino, K. *Tetrahedron Lett.* **2010**, *51*, 4523−4525.

(29) Harb, H. Y.; Collins, K. D.; Garcia Altur, J. V.; Bowker, S.; Campbell, L.; Procter, D. J. *Org. Lett.* **2010**, *12*, 5446−5449.

(30) Erkkila, A.; Pihko, P. M. *J. Org. Chem.* **2006**, *71*, 2538−2541.

(31) This type of scenario also has been observed in terpene-forming carbocation rearrangements; see: Tantillo, D. J. *J. Phys. Org. Chem.* **2008**, *21*, 561−570.

(32) The calculations are consistent with our proposed mechanism but, of course, do not rule out the possibility that other mechanisms are also reasonable.
(33) (a) Becke, A. D. *J. Chem. Phys.* **1993**, *98*, 1372−1377. (b) Becke, A. D. *J. Chem. Phys.* **1993**, *98*, 5648−5652. (c) Lee, C.; Yang, W.; Parr, R. G. *Phys. Rev. B* **1988**, *37*, 785−789. (d) Stephens, P. J.; Devlin, F. J.; Chabalowski, C. F.; Frisch, M. J. *J. Phys. Chem.* **1994**, *98*, 11623−11627. (e) Wheeler, S. E.; Moran, A.; Pieniazek, S. N.; Houk, K. N. *J. Phys. Chem. A* **2009**, *113*, 10376−10384. (f) Pieniazek, S. N.; Clemente, F. R.; Houk, K. N. *Angew. Chem., Int. Ed.* **2008**, *47*, 7746−7749.
(34) For examples of DFT applied to the Prins process, see: (a) Jacolot, M.; Jean, M.; Levoin, N.; van de Weghe, P. *Org. Lett.* **2011**, *14*, 58−61. (b) Alder, R. W.; Carta, F.; Reed, C. A.; Stoyanova, I.; Willis, C. L. *Org. Biomol. Chem.* **2010**, *8*, 1551−1559. (c) Jasti, R.; Rychnovsky, S. D. *J. Am. Chem. Soc.* **2006**, *128*, 13640−13648. (e) Alder, R. W.; Harvey, J. N.; Oakley, M. T. *J. Am. Chem. Soc.* **2002**, *124*, 4960−4961.
(35) Gaussian 09, Revision B.01; Frisch, M. J.; Trucks, G. W.; Schlegel, H. B.; Scuseria, G. E.; Robb, M. A.; Cheeseman, J. R.; Scalmani, G.; Barone, V.; Mennucci, B.; Petersson, G. A.; Nakatsuji, H.; Caricato, M.; Li, X.; Hratchian, H. P.; Izmaylov, A. F.; Bloino, J.; Zheng, G.; Sonnenberg, J. L.; Hada, M.; Ehara, M.; Toyota, K.; Fukuda, R.; Hasegawa, J.; Ishida, M.; Nakajima, T.; Honda, Y.; Kitao, O.; Nakai, H.; Vreven, T.; Montgomery, J. A., Jr.; Peralta, J. E.; Ogliaro, F.; Bearpark, M.; Heyd, J. J.; Brothers, E.; Kudin, K. N.; Staroverov, V. N.; Kobayashi, R.; Normand, J.; Raghavachari, K.; Rendell, A.; Burant, J. C.; Iyengar, S. S.; Tomasi, J.; Cossi, M.; Rega, N.; Millam, J. M.; Klene, M.; Knox, J. E.; Cross, J. B.; Bakken, V.; Adamo, C.; Jaramillo, J.; Gomperts, R.; Stratmann, R. E.; Yazyev, O.; Austin, A. J.; Cammi, R.; Pomelli, C.; Ochterski, J. W.; Martin, R. L.; Morokuma, K.; Zakrzewski, V. G.; Voth, G. A.; Salvador, P.; Dannenberg, J. J.; Dapprich, S.; Daniels, A. D.; Farkas, O.; Foresman, J. B.; Ortiz, J. V.; Cioslowski, J.; Fox, D. J. Gaussian, Inc., Wallingford, CT, 2009.
(36) (a) Fukui, K. *Acc. Chem. Res.* **1981**, *14*, 363−368. (b) Gonzalez, C.; Schlegel, H. B. *J. Chem. Phys.* **1989**, *90*, 2154−2161. (c) Gonzalez, C.; Schlegel, H. B. *J. Chem. Phys.* **1991**, *95*, 5853−5860.
(37) Yanai, T.; Tew, D. P.; Handy, N. C. *Chem. Phys. Lett.* **2004**, *393*, 51−57.
(38) (a) Zhao, Y.; Truhlar, D. *Theor. Chem. Acc.* **2008**, *120*, 215−241. (b) Valero, R.; Costa, R.; Moreira, I.; de, P. R.; Truhlar, D. G.; Illas, F. *J. Chem. Phys.* **2008**, *128*, 114103−114108.
(39) Marenich, A. V.; Cramer, C. J.; Truhlar, D. G. *J. Phys. Chem. B* **2009**, *113*, 6378−6396.
(40) Muller, N.; Falk, A. *Ball & Stick 4.0a12, molecular graphics software for MacOS*, Johannes Kepler University, Linz, 2004.